# The Effect of Wake Models, and Environmental Conditions on Wind Farm Layout Optimization

 $\mathbf{B}\mathbf{y}$ 

#### AMIR DANESHBODI



Aerodynamics, Wind Energy, Flight Performance and Propulsion- Wind Energy Group
DELFT UNIVERSITY OF TECHNOLOGY

A dissertation submitted to the Delft University of Technology in accordance with the requirements of the degree of MASTER OF SCIENCE in the Faculty of Engineering.

February 2018

For my parents. Thanks for always being there for me.

# **ABSTRACT**

The purpose of this research is to broaden current knowledge of Wind Farm Layout Optimization (WFLO). Until now, there are many research conducted on different optimization methods, annual energy yield calculation processes, and wake modeling methods. But, few papers have addressed the effect of different modeling parameters on WFLO in a form of sensitivity analysis. The results would be helpful in order to have a better overview on the effect and importance of each modeling parameters on the objective function calculation which would finally affect the layout found by the optimizer. The first phase of the project defines and categorize parameters affecting the WFLO. The second phase involves setting up the methods to find the effect of the categorized parameters such as turbulence intensity, wind direction sampling step, and wake model selection on WFLO.

The research is done on the analyzer stage and ignored the optimizer. The analyzer has function of calculating the annual energy yield and providing the result to the optimizer module for the WFLO process. Moreover, the study starts from a single wake calculation, to wind farm power production for an individual wind direction, and finally to annual energy yield production. Following these steps is helpful because the same steps happen in the analyzer, and it enables us to determine effects of the parameters within the flow of calculation in the analyzer. These steps are vital to sheds light on the origin of each effect that happens on the annual energy production level and helps to understand if they are magnifying or disappearing during these steps. This study shows that Jensen, Larsen, and Ainslie wake models are similar in ranking the annual energy yield of a wind farm with random configuration, although they have different behaviours in increasing the annual energy production by increasing the spacing in a wind farm (which is more sensible in relatively lower spacing). For instance, in a wind farm with turbines relatively close to each other, the Larsen model has the most increase due to the increase in spacing, which leads the analyzer to find a larger wind farm as the solution (compared to Ainslie and Jensen) when costs (like cabling costs) are also taken into account combined with the annual energy production.

Keywords: Wind farm layout optimization, Analyzer, Optimizer, Sensitivity, Annual energy yield

#### **ACKNOWLEDGEMENTS**

Firstly, I would like to express my sincere gratitude to my advisor, Dr. Michiel Zaaijer, for his continuous support of my study, his patience, encouragement, and broad knowledge. His guidance has helped me throughout doing the whole research and writing of this thesis. He has always been present to keep me motivated and calm during disappointing situations. I could not imagine having a better advisor and mentor for my studies. Also, I would like to thank Ph.D candidate Sebastian Sanchez Perez-Moreno for his kind support during this study. He always helped me with my Python programming issues and generously guided me throughout the technical issues I encountered. My sincere thank also goes to the rest of my thesis committee, Prof. Simon Watson and Dr. Wim Bierbooms, for their insightful comments and encouragement in my mid-term presentation, which incented me to widen my research from various perspectives. I thank our kind academic counsellor, Leonie Boortman, for her support, which means a lot to me. I am thankful to the wind energy group secretary, Sylvia Willems, for her friendly help, to Ph.D candidate Shaafi Kaja Kamaludeen for his advice, and all of my friends who supported me in all the ups and downs of life. Last but not least, I would like to thank my family; my parents, my sister and her husband, and my beloved nephew for supporting me spiritually throughout preparation of this thesis without whom, I believe I could not have continued my graduate studies far from home.

# Nomenclature

# Symbols

$\alpha_1$	calibration coefficient	[m]
$\epsilon$	Eddy viscosity	$[m^2/s]$
$\boldsymbol{A}$	Rotor area	$[m^2]$
$c_1$	Prandtl non-dimensional mixing length	[-]
$D_M$	Center-line speed deficit at 2D	[m/s]
$D_{eff}$	Effective diameter	[m]
$D_r$	Rotor diameter	[m]
$D_w$	wake diameter	[m]
$r_w$	Larsen wake radius	[m]
TI	Turbulence Intensity	[%]
$U_{\infty}$	Upstream wind speed	[m/s]
$U_C$	Ainslie wake center-line velocity	[m/s]
$U_0$	Upstream wind speed	[m/s]
$U_r$	Wind speed at rotor	[m/s]
$U_w$	Wake wind speed	[m/s]
b	Ainslie wake width parameter	[m]
H	Hub height	[m]
X	Axial distance	[m]

# TABLE OF CONTENTS

		<u> </u>	Page
Li	st of	Tables	хi
Li	st of	Figures	xiii
1	Intr	roduction	1
	1.1	Background Information	. 1
		1.1.1 Wind Farm Layout Optimization	. 1
		1.1.2 Wind Farm Model Considering Turbines as Roughness Elements	. 2
		1.1.3 Wind Farm Model using Wake Interactions	. 3
		1.1.4 Wind Resource Assessment Commercial Programs	. 4
		1.1.5 Optimization and Wind Farm Commercial Optimizer	. 5
	1.2	Problem Statement	. 6
	1.3	Objective	. 7
	1.4	Approach	. 7
	1.5	Layout of the Report	. 8
2	Met	hodology and Models	9
	2.1	Overview of Methodology	. 9
	2.2	Affecting parameters	. 9
		2.2.1 Environmental Conditions	. 9
		2.2.2 External Design Parameters	. 10
		2.2.3 Analyzer Design Parameters	. 10
		2.2.4 Investigated Parameters	. 12
	2.3	Study Wake Models' Characteristics	. 12
		2.3.1 Study Method	. 13
		2.3.2 Modeling	. 13
	2.4	Power Output (for individual wind directions)	. 17
		2.4.1 Study Method	. 17
		2.4.2 Modeling	. 19
	2.5	Annual Energy Yield (for the whole wind rose)	. 20
		2.5.1 Study Method	. 20
		2.5.2 Modeling	. 21
3	Res	ults & Discussion	23
	3.1	Results overview	. 23
	29	Waka models characteristics	93

# TABLE OF CONTENTS

	3.3	Wind farm power output	26
	3.4	Wind farm annual energy yield	32
4	Con	clusion & future research	43
	4.1	Conclusion	43
	4.2	Future Research	44
Bi	bliog	raphy	45
A			<b>5</b> 1
В			53
$\mathbf{C}$			55
D			57

# LIST OF TABLES

TAB	SLE F	Page
2.1	Wake summation methods	19
2.2	The used realistic wind-rose	21
3.1	Annual energy yield for the low density $3 \times 3$ wind farm $\dots \dots \dots \dots$	35
3.2	Annual energy production matrix using the Jensen model in the $3 \times 3$ layout. AEPs	
	have been normalized by the computationally most accurate result which is 1 degree	
	direction sampling step and $1m/s$ speed step	37
3.3	Annual energy production matrix using the Larsen model in the $3\times3$ layout. AEPs	
	have been normalized by the computationally most accurate result which is $1\ degree$	
	direction sampling step and $1m/s$ speed step	38
3.4	Annual energy production matrix using the Ainslie model in the $3 \times 3$ layout. AEPs	
	have been normalized by the computationally most accurate result which is 1 degree	
	direction sampling step and $1m/s$ speed step	38
3.5	Annual energy production matrix using the Jensen model in the $10 \times 10$ layout. AEPs	
	have been normalized by the computationally most accurate result which is 1 degree	
	direction sampling step and $1m/s$ speed step	39
A.1	V90-2MW technical specifications	51
D.1	Annual energy production ratio matrix using the Larsen model in the $3 \times 3$ layout.	
	AEPs have been divided by the computationally most accurate result which is 1 degree	
	direction sampling step and $1m/s$ speed step	57
D.2	Annual energy production ratio matrix using the Ainslie model in the $3 \times 3$ layout.	
	AEPs have been divided by the computationally most accurate result which is 1 degree	
	direction sampling step and $1m/s$ speed step	58
D.3	Annual energy production ratio matrix using the Jensen model in the $10 \times 10$ layout.	
	AEPs have been divided by the computationally most accurate result which is 1 degree	
	direction sampling step and $1m/s$ speed step	59

# LIST OF FIGURES

Fig	EURE P	Page	
1.1	Schematic of wind farm layout optimization procedure	2	
1.2	Detailed analyzer schematic	7	
2.1	Schematic of a wind farm from top view - Blue circles represent wind turbine surface after yawing 360 degrees - Top right circles represent the densest wind farm with theoretically 100% density	12	
2.2	Representing the wake expansion profile in Jensen's model and its control volume to	14	
	find wind speed	14	
2.3	Equivalent Jensen's expansion factor for turbulence intensity [63]	15	
2.4	Different cases used in the analysis methodology	18	
<ul><li>2.5</li><li>2.6</li></ul>	Wind farm layout setups	19	
2.7	sampling - b. Same matrix with different starting points	21 22	
3.1	(a) Downstream wake radius for TI = $0.1$ - (b) Downstream wake radius for TI = $0.3$ .	24	
3.2	(a) Downstream wake mean velocity for TI = $0.1$ - (b) Downstream wake mean velocity for TI = $0.3$	25	
3.3	(a) Downstream wake center-line velocity for $TI = 0.1$ - (b) Downstream wake center-		
3.4	line velocity for TI = $0.3$	25	
	directions in the 10 $\times$ 10 layout - (d) The studied layouts	27	
3.5	(a) Power ratio for different wind directions with 8.5 m/s wind speed - (b) Power ratio for different wind directions with 13 m/s wind speed	28	
3.6	(a) Power ratio for different wind directions in the structured layout - (b) Power ratio		
	for different wind directions in the non-structured layout $\ldots \ldots \ldots \ldots$	29	
3.7	(a1) Power ratio for different wind directions in the low density layout and $TI = 0.1$ - (a2) Power ratio for different wind directions in the low density layout and $TI = 0.3$ - (a) Low density layout - (b1) Power ratio for different wind directions in the high density layout and $TI = 0.1$ - (b2) Power ratio for different wind directions in the high		
3.8	density layout and TI = 0.3 - (b) High density layout	30	
	in the $3 \times 3$ layout	33	

3.9	(a) The orange dots shows the added turbine positions, and the blue dots are the base	
	wind farm layout (for the better visualization not the whole farm is shown here) - (b)	
	Wind farm AEP as a function of the added turbine (x) positions in the $10\times10$	34
3.10	Annual energy yield for 8 different random layout with 9 turbines when (a) $TI = 0.1$ ,	
	(b) TI = 0.25	35
3.11	(a1) Ratio of AEPs in figure 3.8 - (b1) Difference of AEPs in figure 3.8 - (a2) Ratio of	
	AEPs in figure 3.10 with TI = 0.1 - (b2) Difference of AEPs in figure 3.10 with TI = 0.3	
	- (a3) Ratio of AEPs in figure 3.10 with TI = $0.1$ - (b3) Difference of AEPs in figure 3.10	
	with TI = 0.3	40
A.1	V90 (a) Thrust coefficient - (b) Power coefficient	51
B.1	Downstream wake radius for TI: $0.1$ and $0.3$ by (a) Ainslie - (b) Jesnen - (c) Larsen	53
B.2	Downstream wake mean velocity for TI: 0.1 and 0.3 by (a) Ainslie - (b) Jesnen - (c)	
	Larsen	54
B.3	Downstream wake center-line velocity for TI: $0.1$ and $0.3$ by (a) Ainslie - (b) Jesnen -	
	(c) Larsen	54
C.1	Downstream wake mean velocity for TI: 0.1 and 0.3 by (a) Ainslie - (b) Jesnen - (c)	
	Larsen	55

# 1

# INTRODUCTION

# 1.1 Background Information

Wind Energy will be one of the main sources of supplying the energy demand in near future; thus, many wind farms should be constructed around the globe. One of the major issues in constructing a wind farm is turbine positioning. Turbine positioning plays an important role due to the impact of turbines on each other. When upstream flow meets a wind turbine, the turbine will slow down the air flow, adds up the turbulence, and also shed wakes in downstream. Regarding these changes in the flow, the downstream turbines will produce less power (due to the velocity, and momentum deficit), and experiencing greater unsteady loads (due to the higher turbulence); So, it is being tried to keep them far from each other. On the other hand, wind turbines should be placed as closely as possible to decrease the land cost, electrical infrastructure cost, electricity transmission losses, operation and maintenance costs [1]. In following sections wind farm layout optimization (section 1.1.1), wind farm modeling (sections 1.1.2, and 1.1.3), and commercial programs for wind resource assessments and optimization (sections 1.1.4, and 1.1.5) are discussed in detail.

#### 1.1.1 Wind Farm Layout Optimization

Finding the minimum Levelized Cost of Electricity (LCoE) of a wind farm requires complex, multi-disciplinary optimization. Most of these issues have been addressed individually as a part of micro-siting problem [2], for instance: wind assessments [3–7], turbines aerodynamics interactions (see section 1.1.2, and 1.1.3), electrical infrastructure [8–10], road route selection [11], reliability [12–14], visual impacts [15–17]. However, in this project, the main focus of the study is on the Wind Farm Layout Optimization (WFLO) only considering the Annual Energy Production (AEP) due to aerodynamic wake losses.

The schematic of wind farm layout optimization is shown in figure 1.1. WFLO procedure starts by setting external conditions such as number of wind turbines and applying the environmental situation like turbulence intensity, and wind-rose. The next step in the procedure is calculating the objective function for the given layout in the analyzer. For instance, the objective function

might be the wind farm annual energy production. So, analyzer will calculate the wind speed at all the turbines in order to calculate the wind farm power output. Afterwards, the analyzer integrates the farm power output for all the wind directions and speeds during a year. Therefore, wake model, wind rose sampling step, and other parameters which will be explained in sections 2.2.1, 2.2.2, and 2.2.3 should be set initially in the analyzer. In the next step, the optimizer will change the layout of the wind farm using different algorithms like "Genetic-based" or "Gradient-based" optimization. So, the objective function of the new layout will be calculated again in the analyzer. This iterative process continues until an optimum layout is found.

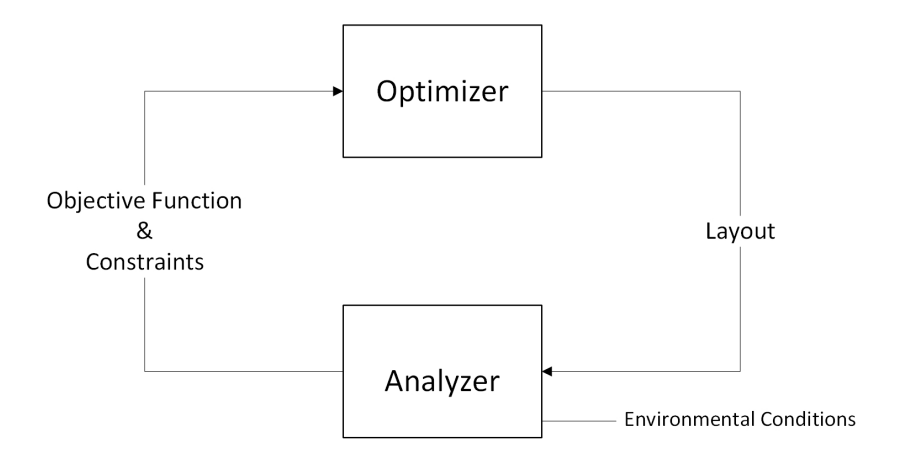


Figure 1.1: Schematic of wind farm layout optimization procedure

Modeling the wind farm for the purpose of calculating the AEP is the main element of WFLO. In general, there are two fundamental approaches to fulfill this need. First, and earlier approach is to consider wind turbines as roughness elements and then by modifying the ambient atmospheric flow, the velocity on each turbine would be calculated (see 1.1.2). Second, and more prevalent approach is wind farm modeling using wake interactions. This method is basically superposing the wake effect of the whole turbines in a farm on each other, and finding the turbines velocity (See 1.1.3). [18]

#### 1.1.2 Wind Farm Model Considering Turbines as Roughness Elements

Regarding this method, Bossanyi et al [19] reviewed several models given by "Templin" [20], "Newman" [21], "Carfoord" [22], and "Moore" [23] that applied to infinite clusters. These models assume a logarithmic wind shear profile for upstream wind by considering the ground roughness. Then each turbine adds up the roughness level which will change the wind profile. At the end, the wind speed and the corresponding power at each turbine will be calculated. Furthermore, Emeis and Frandsen [24] suggested to use two wind profiles, one below the hub with the ground roughness, and one above the hub with the turbine drag. Bossanyi et al [19] also represented a model to extend previous models to finite clusters. It is good to mention that these models are not

frequently used, but they are useful for analyzing the effect of a wind farm on wind condition outside the farm.[18]

#### 1.1.3 Wind Farm Model using Wake Interactions

The most frequent approach for the wind farm modeling is calculating the wake velocity of each turbine, and superposing wake effects of the upstream turbines in order to calculate the rotor velocity, and power generation of each individual turbine in the farm [18]. In this approach having a proper wake model plays a crucial role. Therefore, a detailed background of wake models and wake interaction is given in sections 1.1.3.1, and 1.1.3.2.

#### 1.1.3.1 Wake Models

A comprehensive study of wake aerodynamics is given in [18, 25–30]. It is observed that some models are only acceptable for near wake and other models are accurate for far wake regions [31]. Therefore, wake modeling is divided into two main different categories called near wake and far wake modeling. Near wake refers to right after the blades till 2-4 rotor diameters downstream, which is extremely influenced by the rotor geometry. Far wake is defined as downstream excluding the near wake region which turbulence is the main physical factor in it [32]. It is worth mentioning that turbines should not be placed closer than 2-4 rotor diameters to each other in order to avoid extra fatigue loads caused by other turbines. So, far wake models are more relevant to use in wind farm modeling. In general, there are two different types of far wake modeling. The first sets of modeling are called analytical (empirical, and explicit) models, which are mainly introducing an expression for velocity deficits downstream. Second sets of models are the computational (implicit) models which are solving a flow equation throughout the whole field [31]. Several wake models have been compared in [33], and it has been shown that there is no superiority in accuracy between sophisticated or simplified models. Therefore, empirical models are more common for wind farm calculation due to their lower computational costs for multiple wake modeling. In this project, three different wake models are chosen for conducting the research. The selection was based on the availability of the tools and also covering both explicit and implicit models. Jensen, Ainslie Eddy viscosity, and Larsen are the mentioned models and they are comprehensively introduced in the section 2.3.2

Vanluvanee [34] has compared the factual data of Horns Rev wind farm with the simulated result using Jensen, Ainslie Eddy viscosity, and Larsen using WindPRO software. The results showed that Eddy Viscosity model is more accurate in direct wake power deficit, and less accurate in non-direct wake power deficit. Also, Jensen showed approximately the same results as Eddy Viscosity.

F. Seim [35] has validated Jensen, Larsen, and Ishihara (all three are kinematic models) with the help of WindSim software. In the end, it has been found out that The Ishihara model overestimates the power deficit. The Jensen model also overestimated the peak power deficit, but

lower than Ishihara. Also, the Larsen model was really close to the measured data. And, at the wake centerline, it was clearly the most accurate model.

S. Jeon et al. [36] verified the accuracy of the Eddy Viscosity, Larsen, Jensen, and Frandsen models by comparing to site data. It was shown that the Jensen model is the best model for calculating the centerline wake velocity, and the eddy viscosity and Larsen models are relatively accurate in simulating the wake radius and profile.

EMD International of Denmark has done a comparison between offshore data and three wake models using WindPRO (Larsen, Eddy Viscosity, and Jensen), and they showed that Jensen has the closest results to the actual values [37].

#### 1.1.3.2 Wake Interactions

Wind farms consist of many turbines affecting each other by their wakes. Most of the time, each individual turbine is under influence of several other turbines located upstream; therefore, wake superposition is the main element of transition from single wake modeling to the wind farm modeling. Lissaman [38] assumed the linear superposition of the wake deficit, but this model overestimates the velocity deficit and sometimes it leads to negative velocity. Moreover, Katic [39] introduced the root mean squared of deficits which has the better agreement with the wind tunnel data [39]. More superposition methods have been introduced in the section 2.4.2).

#### 1.1.4 Wind Resource Assessment Commercial Programs

WAsP, WindSim, and Meteodyn are software for wind resource assessments which are also able to calculate the AEP for a given layout. Nevertheless, they are not meant to do the wind farm layout optimization [2].

WAsP [40] is the most known software for wind resource assessments by using nearby meteorological data, or meteorological mast data collected for the measurement campaign. The software calculates the wind resource on the terrain using "micro scale flow analysis". WAsP could calculate energy yield for a single wind turbine or a wind farm, wind farm efficiency, wind resource and turbulence mapping in complex terrain or offshore. Also, it could do the calculation of wind conditions for IEC site assessment for individual wind turbines in a wind farm, e.g. mean wind speed, wind shear, ambient turbulence, extreme wind, and wind flow inclination. It is also worth mentioning that the new version of the software (WAsP 11) is capable of doing wind assessment on a complex terrain, which was not available in previous versions.

WindSim [41] works with the 3D Reynolds-averaged Navier-Stokes principle, solving the non-linear transport equations for mass, momentum, and energy. Designers could find the best points in terms of wind resource (higher wind, and lower turbulence) even in a complex terrain, and in situations with complex local climatology. So, they can find a more desirable area for placing the wind turbines during wind farm design regarding undisturbed wind conditions.

Moreover, WindSim has the AEP module that includes wake effects with the ability of comparing alternative wind farms.

Meteodyn [42] software has a similar function to the previous ones using CFD 3D RANS models. Moreover, it is capable to merge the results with the other provided data from mesoscale analysis. Meteodyn is also able to calculate AEP for a given layout including wake effects.

#### 1.1.5 Optimization and Wind Farm Commercial Optimizer

The optimization generally starts by translating different aspects of a wind farm (AEP, LCOE, noise, and etc.) to a couple of mathematical equation used as objectives and also some constraints [2]. Current optimizers could be divided into three main categories based on their objective functions. The first group just uses the AEP as the objective function, and optimizer tries to maximize it for the wind farm [43]. The second group takes the economic aspect into account and tries to minimize the LCOE. The difference between different tools in this category relates to their cost models [44–55]. For instance, installation costs, operation and maintenance costs, electrical losses, etc. are some of the aspects that affect the LCOE but they might be taken into account or not. Also, the way of translating these costs into the mathematical equation (cost model) will effect the results. The third group is the tools that takes environmental impact of wind farm layout into account as well which makes it even more complicated [56].

Several optimization algorithms have been developed and prosperously implemented to solve wind farm layout design. The most important ones are Genetic Algorithms, Simulated Annealing, Differential Evolution, Simulated Evolution, Ant Colony Optimization, Particle Swarm Optimization, Stochastic Evolution, Definite Point Selection, Bionic Optimization, Gradient-based optimization, Numerical added simulation, and Monte Carlo optimization technique. [31]

Windfarmer, WindPro, and Openwind are commercial software that enable designers to optimize a wind farm [2].

WindFarmer [57] uses Reynolds-averaged Navier-Stokes as the wake solver, and it is maximizing the return of investments; But the details of optimization algorithms and the objective function are not given. Furthermore, Windfarmer is able to compute the noise, visual impact, electrical infrastructure, and uncertainty.

WindPro [58] takes the AEP as the objective function and uses the Katic model for wake analysis [39]. This software allows the user to choose between a random or structured layout. Also, it has a noise module that could be integrated with the optimization to either find the optimum layout and meet the noise constraints.

OpenWind [59] tries to minimize the LCOE. And, it has a different module like shadow flicker, uncertainty estimation, and deep array wake effect using Katic model [39].

It is worth mentioning that the literature on comparing these software and identifying the reasoning of choosing different modeling method in each of them is not as extensive as the literature on different wake modeling methods.

#### 1.2 Problem Statement

Wind farm layout optimization includes two main parts that are analyzer, and optimizer. Setting up a proper analyzer is a fairly complicated process, and requires to be provided with sets of data to implement as environmental conditions. Also, several models exist to analyze the objective function for the optimization (see figure 1.1, see sections 2.2.1, 2.2.2, and 2.2.3). The analyzer part is obliged to calculate the wind velocity field in the wind farm (or the wind velocity at each turbine), the farm power output, and finally the annual energy yield; therefore, different choices for the modeling in the analyzer will end up in different results of the objective function, and thereupon different layouts. For instance, in an optimization, the performance of the wind farm is tested by determining the wake losses for a particular layout of the turbine positions. This assessment is different for different wake models and therefore the optimized positions will differ, depending on the chosen model(s). In the same way, the environmental, and external conditions would have an effect on the analyzer, and respectively on the layout optimization. For instance, by changing the turbulence intensity, the wake model does not represent the same behaviour for the wake velocity which means that the calculated output would be affected by the environmental conditions in a different way for each model. In other words, each parameter in the environmental conditions, or in the implemented model for the analyzer would have an effect on the calculation of wind farm output, and consequently in the wind farm layout optimization. In addition to that, some models are faster to run, and some others are more time consuming which cause a huge computation cost in order to optimize a big wind farm with them. Therefore, the behaviour of the models in different conditions, and under the above-mentioned parameters is an important factor in order to decide to choose between the fidelity level of a model or the speed of it.

There are several parameters that have an impact on the wind farm layout. These factors should be investigated more precisely in order to find their level of influence and importance on the layout. these parameters could be divided into three different categories.

- Environmental conditions
- Design parameters
- Analyzer parameters
- Optimizer parameters

Environmental conditions, design parameters, and analyzer parameters are explained in sections 2.2.1, 2.2.2, and 2.2.3. Optimizer parameters are not discussed in this project and it is out of the scope of this project.

In summary, It is observed that although much is known about wakes and the performance of wake models, little is known about how choices for modeling wakes affect WFLO and optimality.

# 1.3 Objective

The main purpose of this study is to develop an insight for the analyzer (see figure 1.2) in order to find effects on the WFLO. In other words, it is tried to find the sensitivity of the WFLO to each contributed parameters in the modeling. But, effects of optimizer on the WFLO would not be studied in this project due to time limitations. It is tried to step by step clarify the effect of each parameter that is mentioned in sections 2.2.1, 2.2.2, and 2.2.3; first, on the single wake behaviour, second, on the wind farm power output for different wind speeds and directions, and finally, on the annual energy yield. The results would be helpful for us to have a better overview on the effect and importance of each modeling parameters on the objective function of the analyzer which would finally affect the layout found by the optimizer. Furthermore, this study enables us to choose wisely between our modeling options in order to have the best efficiency in the scenes of computation effort, exactness and functionality of the analysis in the framework of layout optimization.

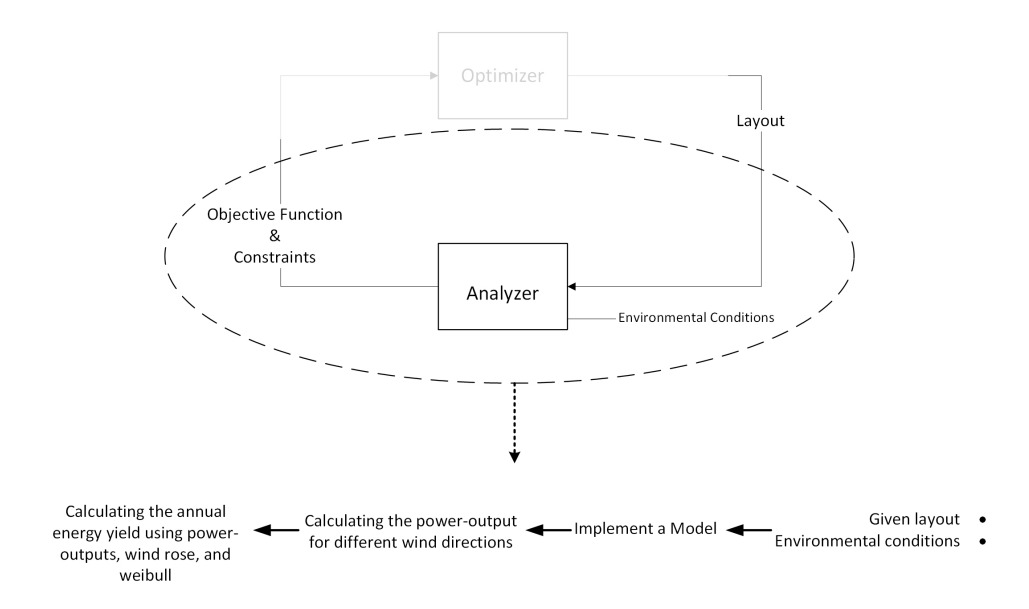


Figure 1.2: Detailed analyzer schematic

# 1.4 Approach

In order to have a better understanding on this complex system, and find the effect of each parameter on the wind farm layout optimization, it is tried to find the sensitivity of different parameters on the analyzer level. Different set-ups and configurations have been generated in "Python" to compare the effect of different parameters while using three different wake models (Jensen, Ainslie, Larsen) which were provided by "Sebastian Sanchez Perez-Moreno" TU Delft Ph.D. candidate. And, the analysis has been taken place in three different levels of comparing the wake models for a single wake situation, comparing the wind farm power output while changing

#### 1. INTRODUCTION

the affecting parameters for the three wake models, and comparing the wind farm annual energy yield by varying the parameters and wake models. Furthermore, detailed steps of study approach are discussed in section 2.

# 1.5 Layout of the Report

Chapter 2 is devoted to describing the important parameters affecting WFLO and introducing setups in which, the effects of each parameter could be realized. In chapter 3, the results and their discussions are shown on the level of wake model characteristics, power output (for individual wind directions), and the annual energy production. Finally, chapter 4 presents the general conclusions driven from the results and later, it gives future research options.

# METHODOLOGY AND MODELS

# 2.1 Overview of Methodology

The analyzer module which is the main subject of research is affected by different parameters. These parameters are divided into three main categories for the purpose of this research. These categories will be introduced and investigated in section 2.2.

In this project, in order to satisfy the research objective, the analysis has taken place into three levels. These levels are concluded from steps shown in figure 1.2 and they are:

- 1. Study wake models' characteristics
- 2. Study wind farm power output for different parameters (for individual wind directions)
- 3. Study wind farm annual energy yield for different parameters (for the whole wind rose)

The above-mentioned steps are explained in sections 2.3, 2.4, and 2.5. So, effects of environmental conditions, external design parameters, and analyzer design parameters are studied in three above mentioned steps.

# 2.2 Affecting parameters

The affecting parameters are divided into three main categories. These categories are environmental conditions, external design parameters, and analyzer design parameters which is explained in sections 2.2.1, 2.2.2, and 2.2.3. Moreover, in section 2.2.4 parameters investigated in the study are mentioned.

#### 2.2.1 Environmental Conditions

There are three different parameters relating to the environmental conditions that affect WFLO. These parameters are:

#### 1. Wind condition and wind rose bin size

Wind condition on a site for upcoming 20 years is not exactly the same as what is predicted in the calculation. So, it is good to figure out, what level of accuracy is logical in the layout optimization while there is uncertainty in the wind. Also, the size of wind bins in the wind rose decrease the accuracy due to the averaging in that specific bin. So, the impact of this parameter on WFLO is a relevant aspect to study.

#### 2. Average wind speed

If the wind speed became higher than the rated wind speed, wake velocity would become greater than rated wind speed in some cases. So, this will not decrease the production of the turbines in the wake. Thus, average wind speed might play a role in the optimization, since this situation may occur more often for higher average wind speeds.

3. Turbulence intensity, and atmospheric stability

Turbulence intensity and atmospheric stability have a complex effect on the wind profile and wind turbine wake behavior which is needful to find their influences on optimization.

## 2.2.2 External Design Parameters

The two parameters that could be categorized in this group are:

#### 1. Density of turbines in the area

The density of a wind farm could be defined as the ratio of the number of wind turbines to the maximum possible number of wind turbines in a given area (see figure 2.1). This parameter is an indicator of how packed turbines are placed in a wind farm. The higher density a wind farm has, the more wake losses accrue. Therefore, wind farm density might be a determining factor in the optimization of turbine positions.

#### 2. Number of wind turbines

The number of turbines in a wind farm has several effects like increasing the wake interactions, increasing wind direction that turbines are aligned, etc.

#### 2.2.3 Analyzer Design Parameters

Several parameters are associated to the modeling choices in the analyzer. These parameters are:

1. Wake model selection, and model parameters

Wake model selection has a lot of influence on the wind farm layout, and there are different considerations which should be taken into account while processing the design. For instance, in the Jensen model the wake expansion factor is needed, however in the Ainslie model turbulence intensity is used. Furthermore, turbine's hub height is one of the inputs in the Larsen model which is not needed in the Jensen or Ainslie (see section 2.3.2).

#### 2. Sampling step for wind directions

In addition to the wind rose bin size effect on the optimization, the sampling angle of the wind directions for the optimization might also play an important role. For instance, the output of the optimization might differ when we use 10-degree sampling step for our calculation or 60-degree step. The former will lead to 36 different directions for optimization wind speed input. But the later only gives 6 directions which seem that has a considerable effect on the AEP calculation, and optimization concurrently.

#### 3. Sampling step for wind speed

The sampling step for the wind speed bin might be an important factor due to the cubic relation of the wind turbine power with the wind speed.

#### 4. Rotor averaged wind speed

The rotor speed profile is not uniform due to several reasons like wind shear, wake radial speed profile, and different wake summations on each point of the rotor (not all wakes cover the whole rotor). There are several approaches to tackle this issue like averaging the wind speed throughout the rotor area or taking the wake mid-point velocity as an average wind speed on the wake area of the rotor and then average it for the whole rotor area. Sebastian Sanchez has been shown that there are not a major difference for different approaches on wind farm power output because the variations cancel each other out, and the second approach which is faster has an acceptable accuracy compared to the first approach [60].

#### 5. Wake mixing/summation

In a wind farm, most of the times several wakes of different turbines mix with each other downstream. So, having a proper model for wake summation is really important and the modeling choices in this section might influence the result.

#### 6. Increased turbulence intensity due to wakes

Each turbine causes an increase in the turbulence intensity of the flow generally in its wake. So, the re-energizing rate of wake flow will increase in this situation. This phenomenon has an effect on the power output and AEP respectively.

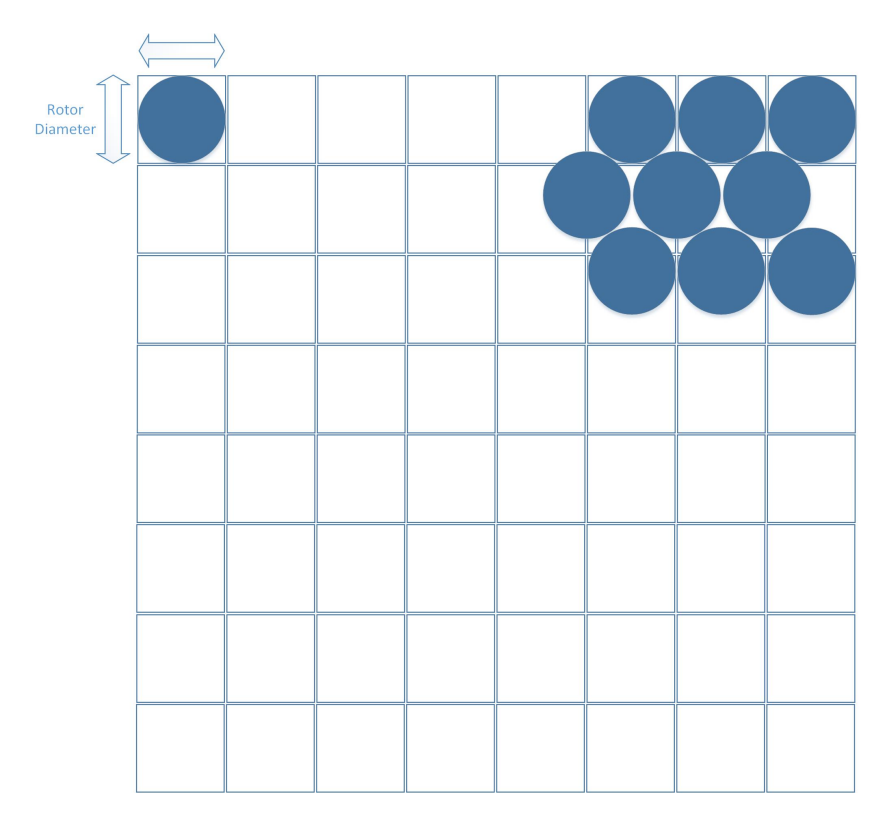


Figure 2.1: Schematic of a wind farm from top view - Blue circles represent wind turbine surface after yawing 360 degrees - Top right circles represent the densest wind farm with theoretically 100% density

#### 2.2.4 Investigated Parameters

In this project, not all of the parameters are investigated. From the environmental conditions (section 2.2.1) only average wind speed and turbulence intensity are studied. In the external design parameters (section 2.2.2) both density of turbines and number of turbines are examined during the research. Relating to the analyzer design parameters (section 2.2.3), wake model selection, wind direction sampling step, and wind speed sampling step effects are studied. Moreover, wake summation is not investigated; because in literature, the best choice for modeling is given (see section 2.4.2). Furthermore, the rotor averaging for the wind speed is performed with only one selected approach (see section 2.2.3) due to the reason that is explained earlier. Also, it is good to mention that increased turbulence intensity due to wakes are neither studied nor implemented in the modeling for this research.

# 2.3 Study Wake Models' Characteristics

Wind energy assessment that is "a game of inches in which percentage points means differences in ten of millions of dollars"[31]. Wake model selection is the main part of the wind farm layout design process which is contributed to the analyzer (see figure 1.1), and it is important, because

the aerodynamic power loss is directly related to the wake losses. Moreover, re-energizing rate of the flow and wake expansion profile are expressed differently for different models. Therefore, the wake model is highly influential on the wind energy assessment. In section 2.3.1 the method of analyzing wake models' characteristics is introduced, and in section 2.3.2 details of used wake models is given in order to find better vision about the physics, and mathematics behind each models, and their behaviour.

#### 2.3.1 Study Method

Based on the mentioned content in section 1.1.3.1, and the importance of wake model selection; three different methods for wake modeling have been chosen to roughly cover a suitable range of kinematic and field models [31]. Selected wake models are:

- N.O. Jensen wake model
- · Eddy viscosity wake model by Ainslie
- · G.C. Larsen wake model

In order to do this analysis, wake center-line velocity, wake mean velocity, and wake radius for different turbulence intensities should be calculated for all the chosen models. Wake mean velocity is defined as the averaged velocity over the wake radius.

#### 2.3.2 Modeling

N.O. Jensen, Ainslie, and G.C. Larsen wake models are going to be explained elaborately in 2.3.2.1, 2.3.2.2, and 2.3.2.3.

#### 2.3.2.1 N.O. Jensen's wake model

The Jensen's model is one of the earliest wake models and it is frequently used in modeling due to its simplicity and speed. This model assumes that wake expands linearly after the wind turbine and then apply continuity equation to a control volume that is visualized in figure 2.2 in order to find the wake wind speed in each axial position downwards [32] according to:

$$\left(\frac{D_r}{2}\right)^2 \cdot U_r + \left[\left(\frac{D_w}{2}\right)^2 - \left(\frac{D_r}{2}\right)^2\right] \cdot U_0 = \left(\frac{D_w}{2}\right)^2 \cdot U_w$$

In which  $D_r$  is the rotor diameter,  $D_w$  is the wake diameter at a certain axial position behind the rotor, and  $u_r$ , and  $u_w$  are the wind speed immediately after the rotor and in the wake respectively. By using the axial induction factor and its relation to the thrust coefficient  $(C_T)$  the wake speed as a function of axial distance (x) is given by equation 2.2

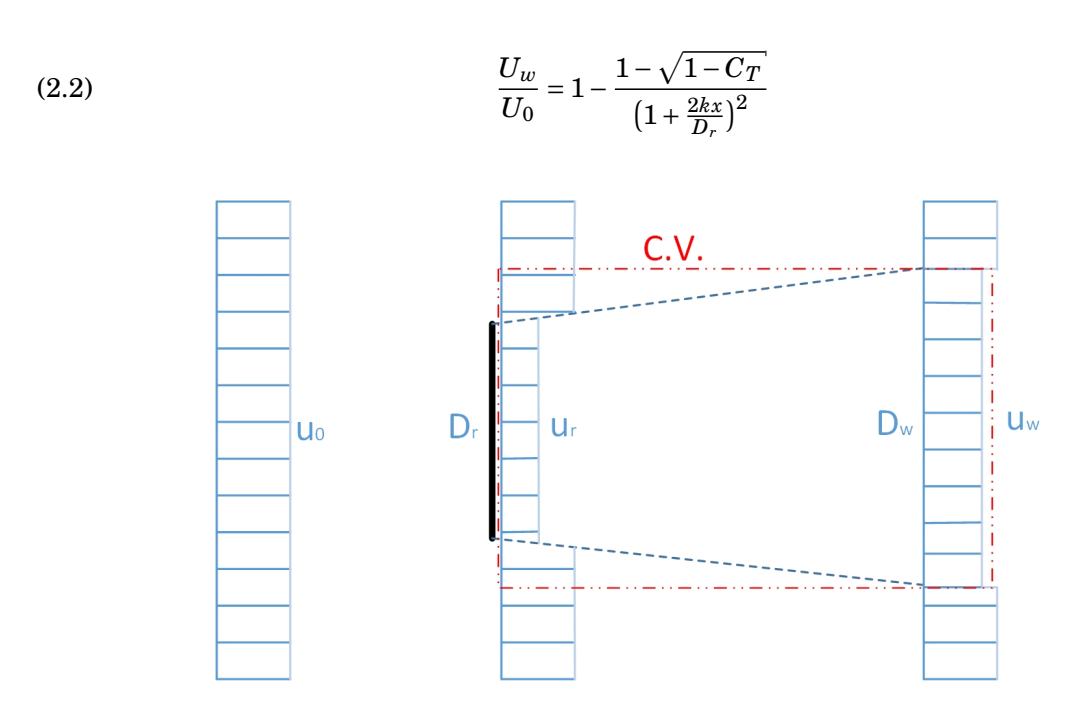


Figure 2.2: Representing the wake expansion profile in Jensen's model and its control volume to find wind speed

It should be mentioned that the Jensen model completely ignores the near wake flow details, so it should be valid beyond the distance  $2-4D_r$  behind the rotor. [60]

#### Relation between Jensen's expansion factor and turbulence intensity

As it was mentioned in 2.3.2.1, the Jensen model uses an expansion factor for the wake. This expansion factor is highly related to the turbulence intensity of the environment [61] and the relation between Jensen expansion factor and turbulence intensity is given by equation 2.3 [62]. However, a more precise model is shown in figure 2.3 [61] [63].

$$(2.3) k = 0.4 \times TI$$

Equation 2.3 is important due to its ability to change the input of the Jensen program from the expansion factor, to turbulence intensity. Also, this enables the comparison ability with other models that use turbulence intensity as an input.

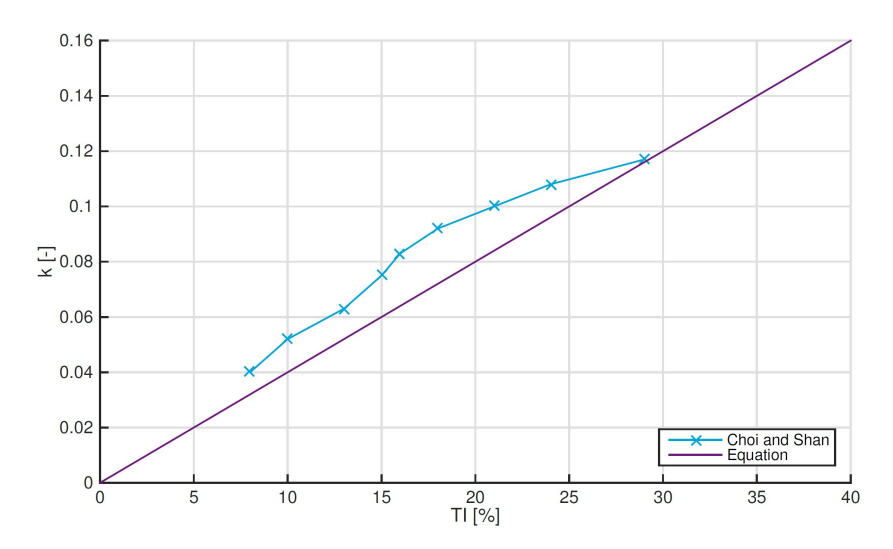


Figure 2.3: Equivalent Jensen's expansion factor for turbulence intensity [63]

#### 2.3.2.2 Eddy viscosity wake model by Ainslie

Ainslie's model includes more actual flow physics compare to empirical models (for example Jensen). It solves a thin shear layer approximation of the Navier-Stokes equation and neglects viscous effects. Using Reynolds stress definition for the turbulence viscosity and the continuity equation a differential equation could be set up for the whole domain. By providing a Gaussian wake profile at 2D downstream (which is experimentally concluded)[64], and knowing the fact that the Ainslie equations produce a self-similar Gaussian shape downstream, the wake velocity anywhere in the grid could be calculated just by finding the center-line velocity [65] through:

(2.4) 
$$U = U_{\infty} \left( 1 - D_M \times e^{-3.56 \left( \frac{r}{b} \right)^2} \right)$$

Where  $D_M$  is the center-line speed deficit and its value for the 2D behind the rotor base on the experimental data is:

(2.5) 
$$D_{M_{2D}} = C_T - 0.05 - (16C_T - 0.5) \frac{TI}{1000}$$

and b is the wake width parameter which is derived from conservation of momentum:

(2.6) 
$$b = \sqrt{\frac{3.56C_T}{8D_M(1 - 0.5D_M)}}$$

Center-line velocity could be calculated with a simple numerical integration of the first order differential equation shown below:

(2.7) 
$$\frac{dU_c}{dx} = \frac{16\epsilon(U_c^3 - U_\infty U_c^2 - U_\infty^2 U_c + U_\infty^3)}{U_c C_T}$$

So, other velocities would be found with the fact that the wake has an identical Gaussian shape, and the differences are just in width and depth which could be found with the equations 2.6, and 2.7.

#### 2.3.2.3 G.C. Larsen's wake model

G.C. Larsen's wake model Applies Prandtl's turbulent boundary layer equations assuming large Reynolds number. The flow is assumed to be incompressible, stationary, and wind shear is neglected [66][60]. After further calculation and assumption, wake radius and wake velocity deficit are:

(2.8) 
$$r_w = \left(\frac{35}{2\pi}\right)^{\frac{1}{5}} (3c_1^2)^{\frac{1}{5}} (C_T A x)^{\frac{1}{3}}$$

$$(2.9) U_x = -\frac{U_\infty}{9} (C_T A x^{-2})^{\frac{1}{3}} \left[ r^{\frac{3}{2}} (3c_1^2 C_T A x)^{-\frac{1}{2}} - \left( \frac{35}{2\pi} \right)^{\frac{3}{10}} (3c_1^2)^{-\frac{1}{5}} \right]^2$$

In which A is rotor area and  $c_1$  is the prandtl non-dimensional mixing length that is given by:

(2.10) 
$$c_1 = \left(\frac{D_{eff}}{2\alpha_1}\right)^{\frac{5}{2}} x_0^{-\frac{5}{6}}$$

Where  $\alpha_1$  is calibration coefficient, and  $D_e f f$  is effective diameter:

(2.11) 
$$\alpha_1 = (\frac{105}{2\pi})^{\frac{1}{5}} (C_T A)^{\frac{1}{3}}$$

(2.12) 
$$D_{eff} = D \sqrt{\frac{1 + \sqrt{1 - C_T}}{2\sqrt{1 - C_T}}}$$

 $x_0$  is:

(2.13) 
$$x_0 = \frac{9.5D}{\left(\frac{2R_{9.5}}{D_e f f}\right)^3 - 1}$$

 $R_{9.5}$  is the radius of the wake at 9.5D downstream and is given by:

$$(2.14) R_{9.5} = 0.5[R_{nb} + min(H, R_{nb})]$$

In which H is hub height.  $R_{nb}$  is given by:

$$(2.15) R_{nb} = max(1.08D, 1.08D + 21.7D(TI - 0.05))$$

## 2.4 Power Output (for individual wind directions)

The second step in the analyzer is calculating the wind farm power output for each specific wind direction; therefore, studying effects of different parameters on this step is necessary and useful to better understand the WFLO. In section 2.4.1, different configurations of parameters have been chosen to be analyzed using the wake models to compare their effects on the power output. In section 2.4.2, the main challenge in calculating wind farm power output, that is wake superposition, is discussed.

#### 2.4.1 Study Method

In order to have an easier comparison between the effect of different parameters while using different wake models, a specific setup is used in this project. In general, the setup has been designed in a way that turbulence intensity, density, number of turbines, and layout structure are varying respectively within two main scenarios. The scenarios are:

#### 1. Wind direction

Calculating the wind farm power output for a specific wind direction and repeating the calculation to cover the whole 360 degrees.

#### 2. Wind speed

Calculating the power output using two different wind speeds.

As shown in figure 2.4, the scenarios will be calculated using the three chosen wake models. Furthermore, the calculation will be repeated for different densities and turbulent intensities within structured or non-structured layouts.

By calculating all the above-mentioned configurations, the sensitivity of the result to density, number of turbines, having a structured or non-structured layout, and turbulence intensity

within different wake models will be found. Furthermore, it gives a good indication about effects of parameters on other parameters' sensitivity.

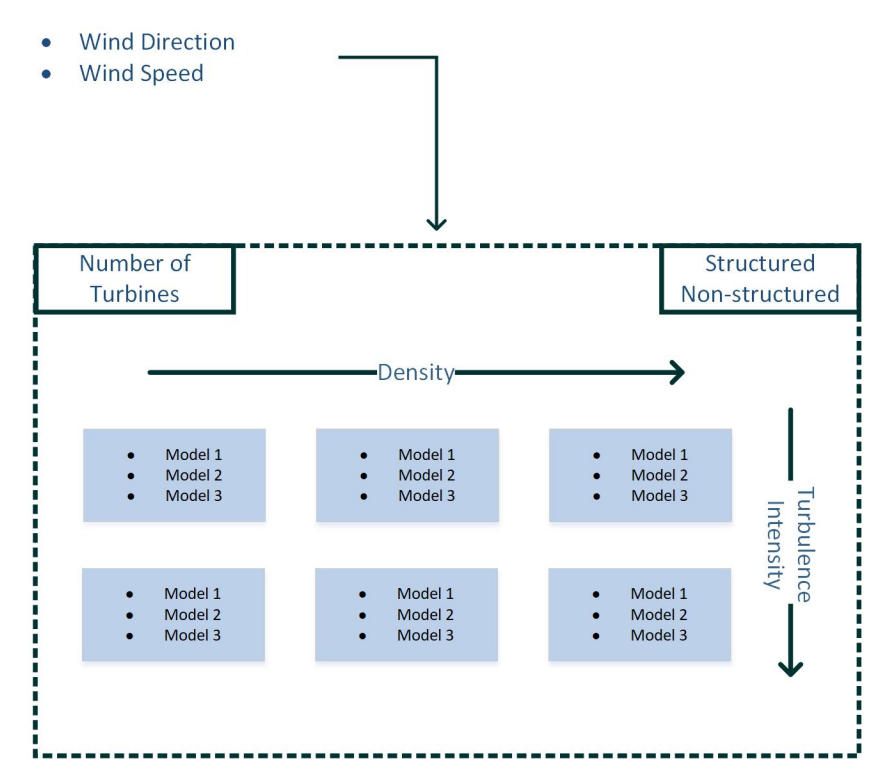


Figure 2.4: Different cases used in the analysis methodology

The following layouts have been used (also see figure 2.5):

- $3 \times 3$ ,  $6 \times 6$ , and  $10 \times 10$  structured layout with [2D,4D] <sup>1</sup>, [4D,6D], and [6D,8D] spacing
- 6 randomly placed wind turbines with almost same overall density as previous item.

 $<sup>^{1}\</sup>mathrm{This}$  means that turbines placed with 2D distance in x-direction, and 4D distance in y-direction from their neighbours

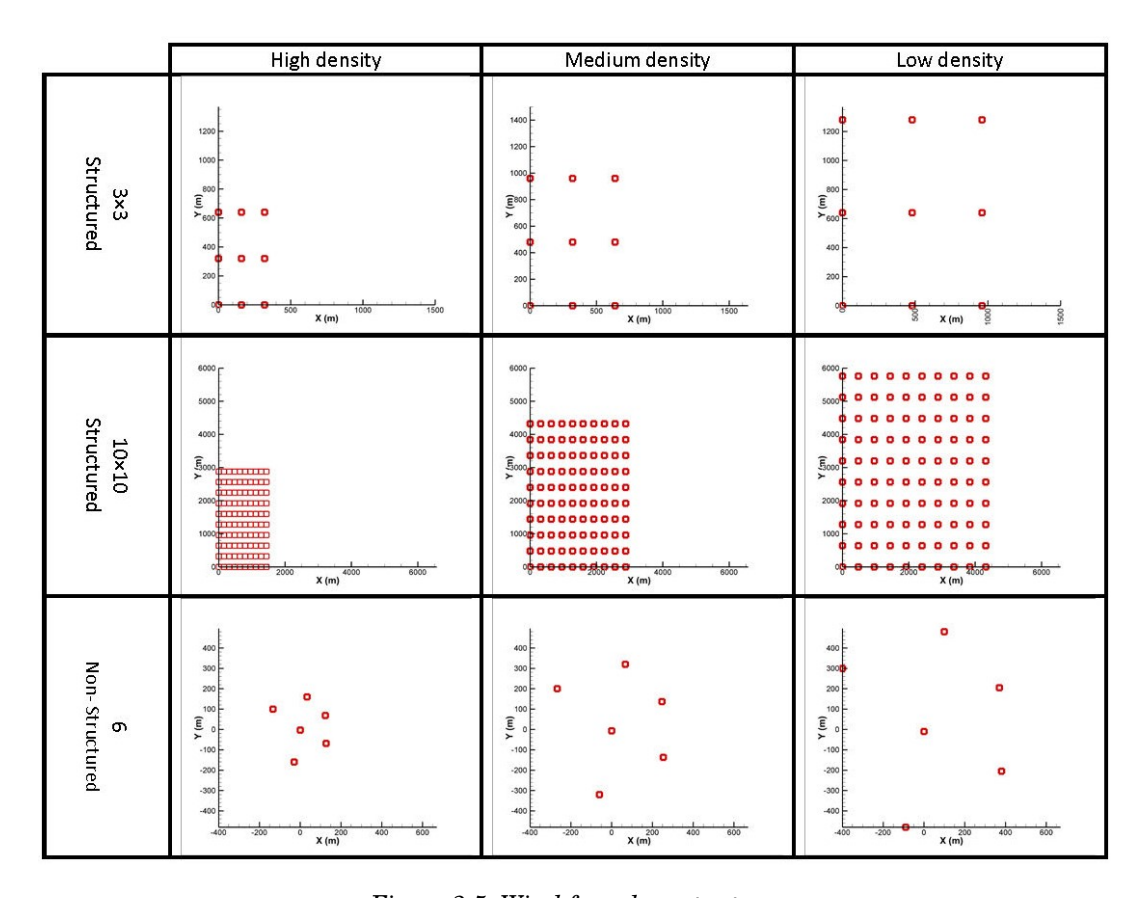


Figure 2.5: Wind farm layout setups

For the turbulence intensity, the upper limit and lower limit of Choi, and Shan (see figure 2.3) [61], which are 0.1 and 0.3, are used. Although TI = 0.3 is high, it has been used to magnify the effect of turbulence intensity on the power production.

#### 2.4.2 Modeling

In order to calculate the power output of a wind farm, a proper model for wake superposition is needed. Several mathematical methods for wake summation are given in table 2.1 [33].

Table 2.1: Wake summation methods

 $\begin{array}{ll} \text{Geometric sum} & \frac{u_i}{u_\infty} = \prod_j \frac{u_{ij}}{u_j} \\ \text{Linear summation} & 1 - \frac{u_i}{u_\infty} = \sum_j (1 - \frac{u_{ij}}{u_j}) \\ \text{Energy balance} & u_\infty^2 - u_i^2 = \sum_j (u_j^2 - u_{ij}^2) \\ \text{Root mean square} & (1 - \frac{u_i}{u_\infty})^2 = \sum_j (1 - \frac{u_{ij}}{u_j})^2 \\ \end{array}$ 

In table 2.1  $u_i$  is wind speed at rotor i,  $u_{ij}$  is the wind speed at rotor i due to (the wake of) rotor j. E. Djerf and H. Mattsson showed that the sum of squares method is the most accurate method for nearly all situations, followed by an energy balance [67]. Moreover, WindFarm developers do

not advise using the methods geometric sum and linear superposition, due to their overestimation in velocity deficit. It is worth mentioning that the sum of squares method is the only possible wake summation method in WindPRO [33]. Also, in this project, only the sum of squares method is used, because it is proven that this the is best available option for the modeling.

## 2.5 Annual Energy Yield (for the whole wind rose)

The third and last part of the analyzer is calculating the annual energy production. In this section, it is tried to describe the analysis method for the parameters' effects on the AEP. Therefore, in section 2.5.1, proper setups for the analysis are introduced. In section 2.5.2 modeling considerations and techniques are explained.

#### 2.5.1 Study Method

In the last part of the analyzer, annual energy production of a specific layout will be calculated. Therefore, this is the most important part for the analysis of WFLO in the scope of this project. This part is important, because the integration of the whole wind farm for all wind directions might cause the effects that occurs in the previous stages to cancel each other out, or magnify. So, this step is crucial to study, but due to the time-consuming runs, limited cases have been studied in this project.

First, the AEP will be calculated for the whole wind farm when an extra turbine is introduced in it. Then the added turbine will be moved through a certain curve (sinusoidal curve in this case) and AEP is plotted for turbine positions along this line. The behavior of the results for different wake models is a good indication of the behavior of the models in the case of optimization in which all the turbines will be moved in order to find the most efficient layout. Again, the low density  $3\times3$  structured layout with the low turbulence intensity is used for the analysis and all the three wake models are compared in this setup. Also, the low density  $10\times10$  structured layout is used with Jensen and Larsen model to also check the effect of number of turbines in a wind farm. Ainslie, is not used in the later setup due to its high computation time.

Second, 9 turbines placed randomly in a square with  $12D \times 12D$  dimensions. In order to avoid the accumulation of all the turbines in a single place, the ground is divided into 9 sub-grids  $(4D \times 4D)$ , and forced that each sub-grids consist one turbine. In this setup, 8 different random layouts are generated, and the AEP is calculated for all of them using all three models. This setup would be a good connection from the analyzer to the optimizer, because the optimizer perform similar action during the WFLO.

Third, the effect of wind direction sampling step and wind speed sampling step on the result will be studied with all three wake models. Also, the starting points of wind direction sampling have been changed in order to study the effect of this choice. The details of this setup are shown

in figure 2.6. Moreover, in this analysis only the low density  $3 \times 3$  structured layout with two different turbulence intensities (0.1, and 0.3) is used.

	30	10	5	1	Wind direction sampling step [°]
	0	0	0	0	Direction sampling starting point [°]
Wind speed sampling frequency [m/s]					
1					
3					
7					
21					

(a)

	30	10	5	1	Wind direction sampling step [°]
	15	5	2.5	0.5	Direction sampling starting point [°]
Wind speed sampling frequency [m/s]					
1					
3					
7					
21					

(b)

Figure 2.6: a. AEP calculation matrix with zero degree (north) starting point of wind direction sampling - b. Same matrix with different starting points

## 2.5.2 Modeling

The wind condition for the AEP calculation is modeled by a realistic wind rose with 30 degrees bin size that is shown in table 2.2. Each section is defined with three numbers which are Weibull scale factor, Weibull shape factor, and probability of occurrence of the wind in that specific bin in a year.

Table 2.2: The used realistic wind-rose

Wind direction	Scale factor	Shape factor	Probability
0	8.65	2.11	5.1
30	8.86	2.05	4.3
60	8.15	2.35	4.4
90	9.98	2.55	6.6
120	11.35	2.81	8.9
150	10.96	2.74	6.5
180	11.28	2.63	8.7
210	11.5	2.4	11.5
240	11.08	2.23	12.1
270	10.94	2.28	11.1
300	11.27	2.29	11.4
330	10.55	2.28	9.6

Calculating the AEP starts by setting a value for "wind direction sampling step" and "wind speed sampling step". In each direction sample, the probability of occurrence is calculated using Weibull function. Moreover, sampling of the wind direction might be started from an angle different from zero. An example of this is given in figure 2.7. Also, the difference between the wind-rose bin size and sampling step is shown in figure 2.7. It should be mentioned that sampling frequency and wind-rose bin size are accidentally equal in this figure which might not be same in the process.

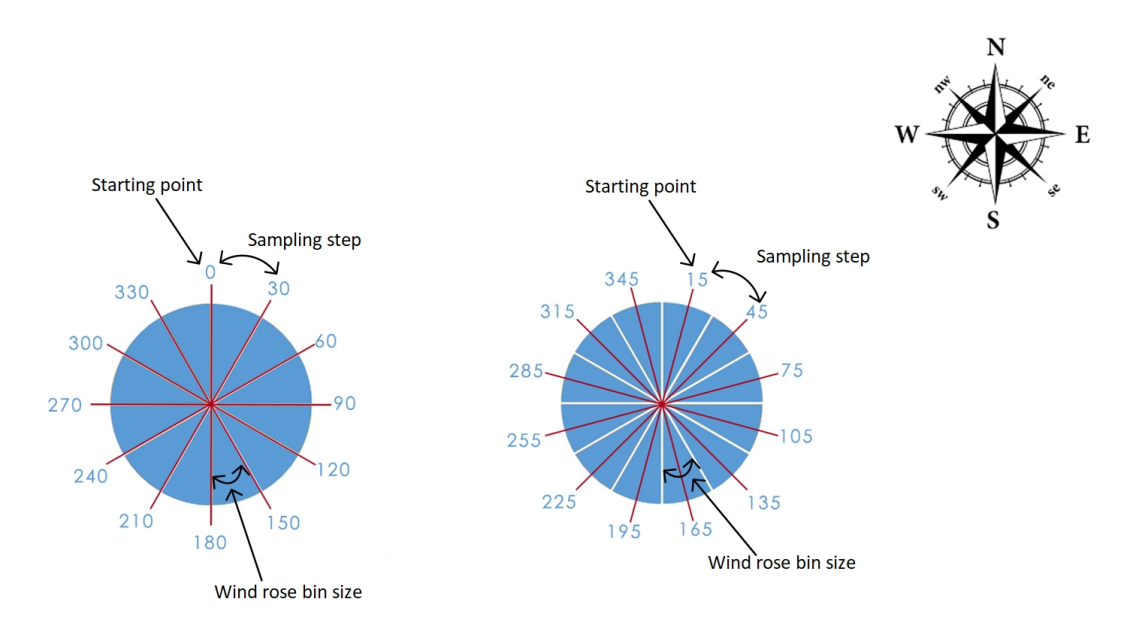


Figure 2.7: Two different starting points for the wind direction sampling in a uniform wind-rose

# 3

## **RESULTS & DISCUSSION**

#### 3.1 Results overview

In this chapter the results for the setups explained in chapter 2 are given in the same logical order. This structure is taken from the analyzer calculation order; therefore, it highlights effects of the parameters from the preliminary stage of wake calculation to the final stage of annual energy yield estimation. Single wake model characteristics, wind farm power output, and wind farm annual energy yield results are established in 3.2, 3.3, and 3.4.

#### 3.2 Wake models characteristics

Looking at wake radius, wake mean velocity, and wake center-line velocity of different models in figures 3.1, 3.2, and 3.3 would be constructive to better understand the behaviour of each model in calculating the power output of a wind farm for different wind directions. It is really important to mention that comparing the exact numbers of wake radius and wake mean velocity is not a reasonable action. Because, each model gives a specific definition of wake radius which makes it irrelevant to just compare the numbers in them. The better approach to analyze these two figures is to analyze the general trends instead of the numbers. It should be mentioned that figures B.1, B.2, and B.3 in Appendix B show the same graph as figures 3.1, 3.2, and 3.3, but organized differently to identify differences of each model for different turbulence intensity.

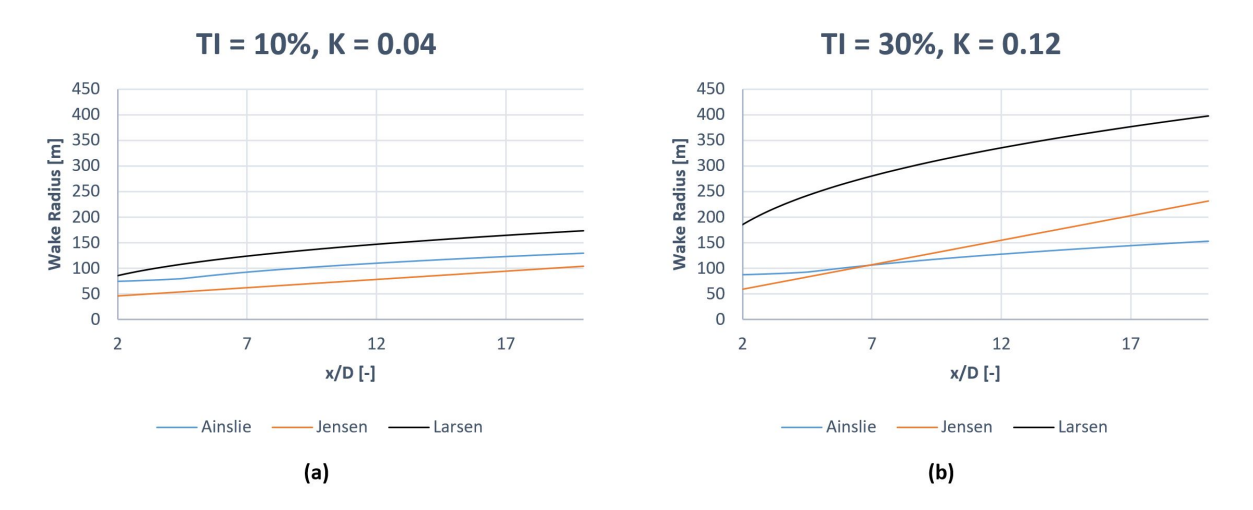


Figure 3.1: (a) Downstream wake radius for TI = 0.1 - (b) Downstream wake radius for TI = 0.3

## Figures 3.1 and B.1 revealed that:

- The models, wake radius increases by increasing TI; however, they have different patterns of increasing. For the Jensen model, just the wake radius slope increases, Ainslie has a small-scale shift upward, and Larsen has both an increase in the slope and a large-scale shift upward. Moreover, the Jensen wake radius growth with TI is more visible far from the rotor. Because, it just has a higher slope with the same radius at the rotor.
- Larsen shows a drastic wake radius growth with TI unlike Ainslie that has only a slight shift upward.
- However the Jensen wake radius is the smallest for the TI = 0.1 among the other models, Small expansion of the Ainslie wake radius causes the Jensen wake radius become larger than Ainslie after 7D for TI = 0.3.

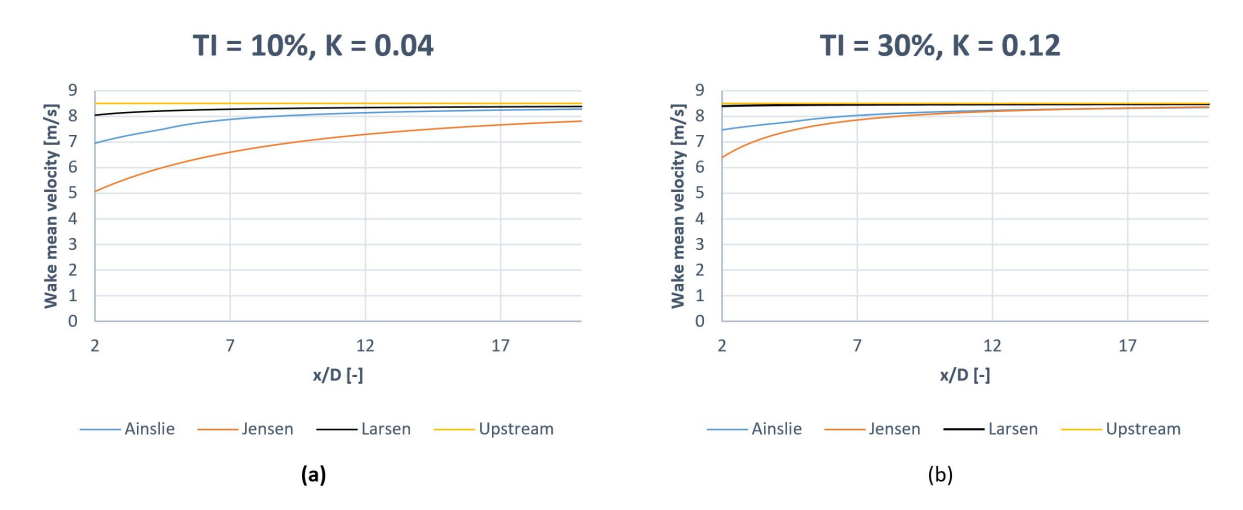


Figure 3.2: (a) Downstream wake mean velocity for TI = 0.1 - (b) Downstream wake mean velocity for TI = 0.3

Looking at figures 3.2 and B.2 show that:

- Larsen has the highest wake mean velocity (for both high and low TI) as a result of considering a relatively long width as its wake.
- Ainslie has the lowest increase by TI compare to the other models (also see figure.
- Wake mean velocities of all the models (regardless of TI) are more similar in far distances than near distances.

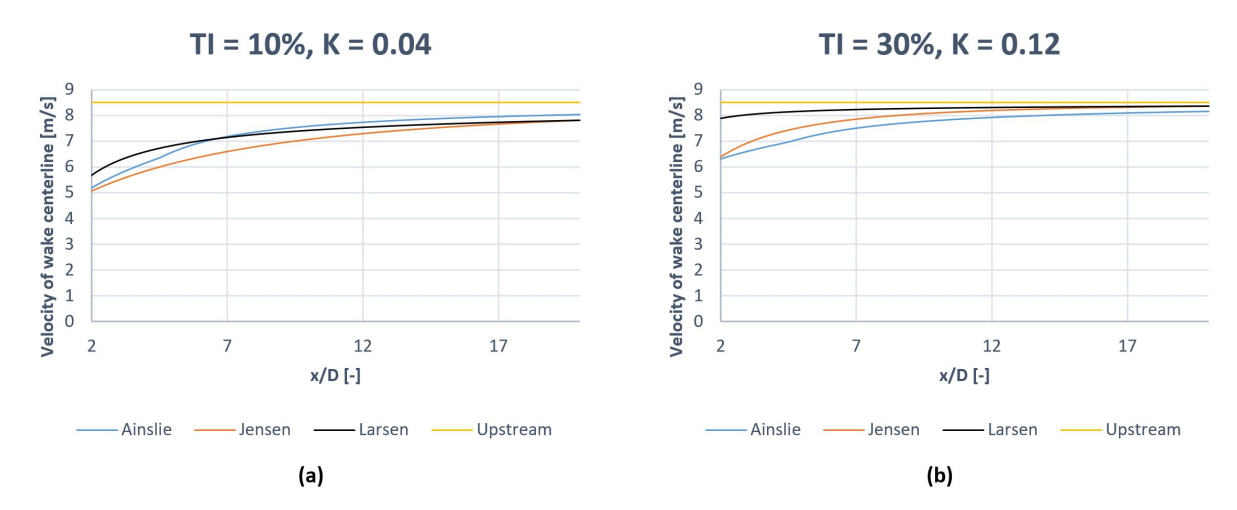


Figure 3.3: (a) Downstream wake center-line velocity for TI = 0.1 - (b) Downstream wake center-line velocity for TI = 0.3

Figures 3.3 and B.3 identified that:

- Larsen has the highest increase in center-line velocity by TI, and Ainlsie has the lowest increase.
- In the lower TI models have more similar center-line velocity than the higher TI.
- The TI = 0.1, Ainslie has higher center-line velocity compare to Larsen after 6D. However, Ainslie has the lowest center-line velocity for the TI = 0.3 compare to the others.
- Wake center-line velocities of all the models (regardless of TI) are more similar in far distances than near distances.

The remarkable conclusion from figures 3.1, 3.2, and 3.3 is that the Ainslie model is the least sensitive model to TI and the Larsen model has a more pronounced change with TI. Moreover, when the Larsen model is used, the optimized layout may depend more on TI, while for the other models the optimized layout may be less sensitive to TI. Also, using Jensen's model for the high TI, may lead to larger spacing because it has larger increase in wake mean velocity and wake center-line velocity for increasing spacing. Also, for the same reasoning Jensen is more sensitive when turbines are relatively close (Less than 3D) which is more noticeable for larger TI.

## 3.3 Wind farm power output

The setup shown in figure 3.4(d) has been analyzed in order to clarify the effect of the number of turbines in a wind farm. With regards to this objective, three different layouts with  $3 \times 3$ ,  $6 \times 6$ , and  $10 \times 10$  structures with the low density spacing are used. The graphs show the power ratio of the farm for each single wind direction. Power ratio is defined as the calculated power output divided by the maximum output without any wake losses.

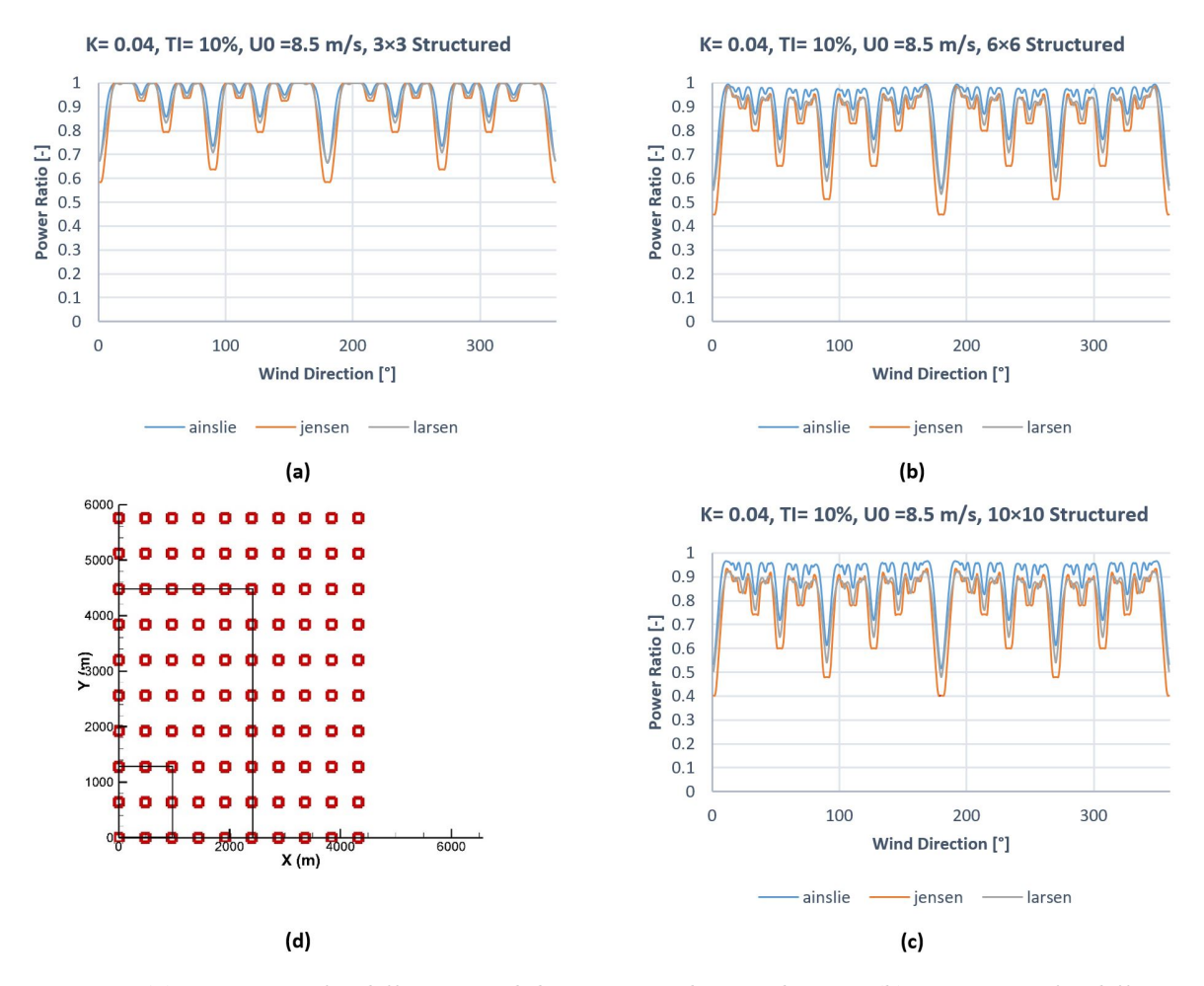


Figure 3.4: (a) Power ratio for different wind directions in the  $3\times3$  layout - (b) Power ratio for different wind directions in the  $6\times6$  layout - (c) Power ratio for different wind directions in the  $10\times10$  layout - (d) The studied layouts

#### Main points observed in figure 3.4 are:

- Generally, the power losses increase by increasing number of turbines.
- The more turbines a wind farm has, the more directions that turbines become in the wake of each other. Basically, by selecting each two turbines, there is a direction of wind that wake losses occurs. Therefore, larger wind farms have more directions with power ratio less than 1.
- Comparing the 6 × 6 with the 10 × 10 layout illustrates the fact that after a relatively long distance, turbines have a negligible effect on each other. Comparing the power ratio in some directions with a lot of turbines in a row, for instance, 180 degrees, clarifies that the power ratio for both layouts are more or less the same in this direction which was relatively higher in the 3 × 3 layout.

By comparing the power ratio of the  $3 \times 3$  layout for two different wind speeds of 8.5 m/s and 13 m/s, the effect of wind speed is spotlighted. The result is depicted in figure 3.5.

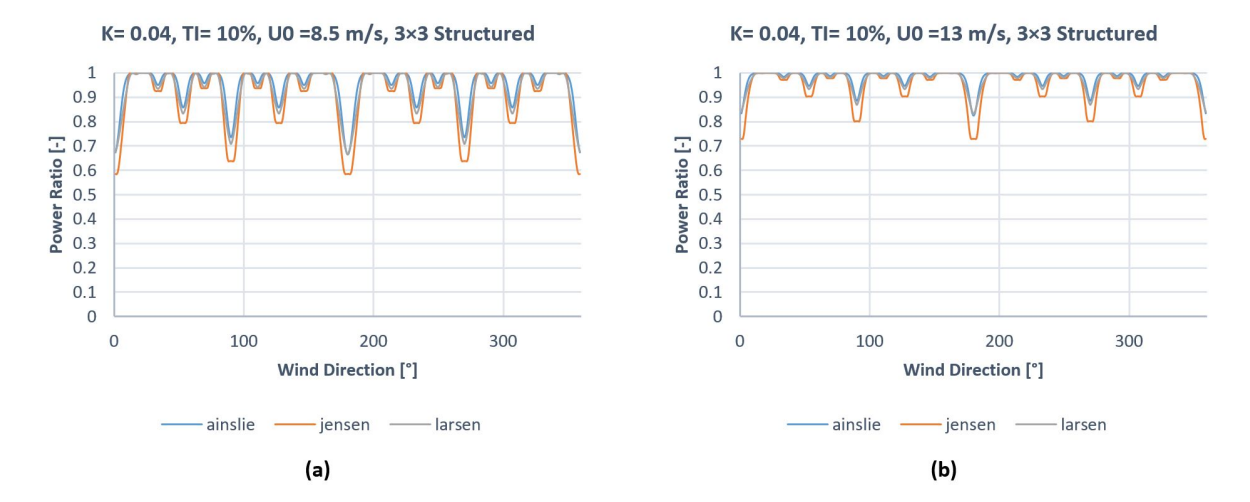


Figure 3.5: (a) Power ratio for different wind directions with 8.5 m/s wind speed - (b) Power ratio for different wind directions with 13 m/s wind speed

#### Main points of figure 3.5 are:

- The power ratio is higher for 13 m/s wind speed. This is because the wind turbines'  $C_t$  decreases by increasing the wind speed (see appendix A). Therefore, the wake deficit and power ratio will be lower for the higher wind speeds.
- For wind speeds higher than rated wind speed, there would be a chance that the wind speed in wake is still higher than the rated speed. Therefore, the power ratio might be higher for relatively high wind speeds.

In figure 3.6, the power ratio for two structured and non-structured layouts with a nearly equal density is shown.

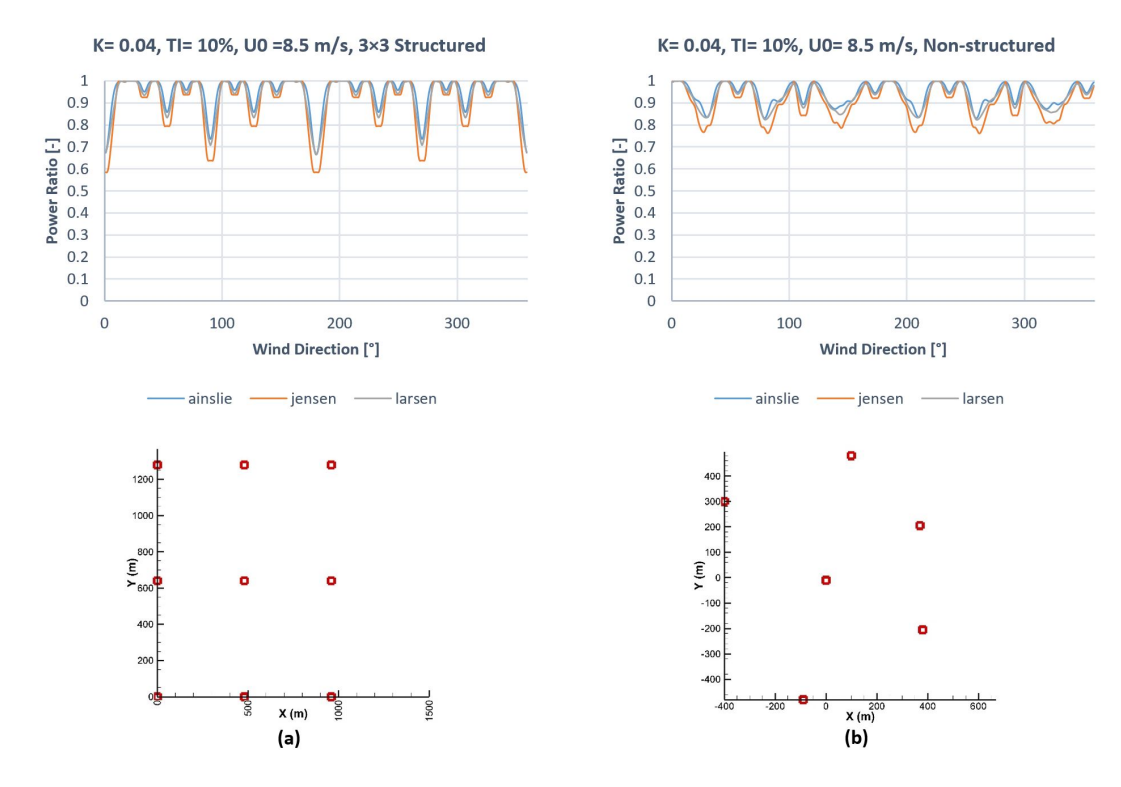


Figure 3.6: (a) Power ratio for different wind directions in the structured layout - (b) Power ratio for different wind directions in the non-structured layout

Comparing the power ratio difference between the structured and non-structured layout (in figure 3.6) shows that:

• in non-structured layouts the power ratio curve is less peaked and has a smaller range of variation; because, the turbines are distributed in a more scattered way. While, in structured layouts there are some directions which a lot of turbines are aligned with each other and some directions with relatively less turbines aligned.

In order to find the density, and turbulence intensity effects, the calculations have been done for high and low density with two different turbulence intensities (see figure 3.7).

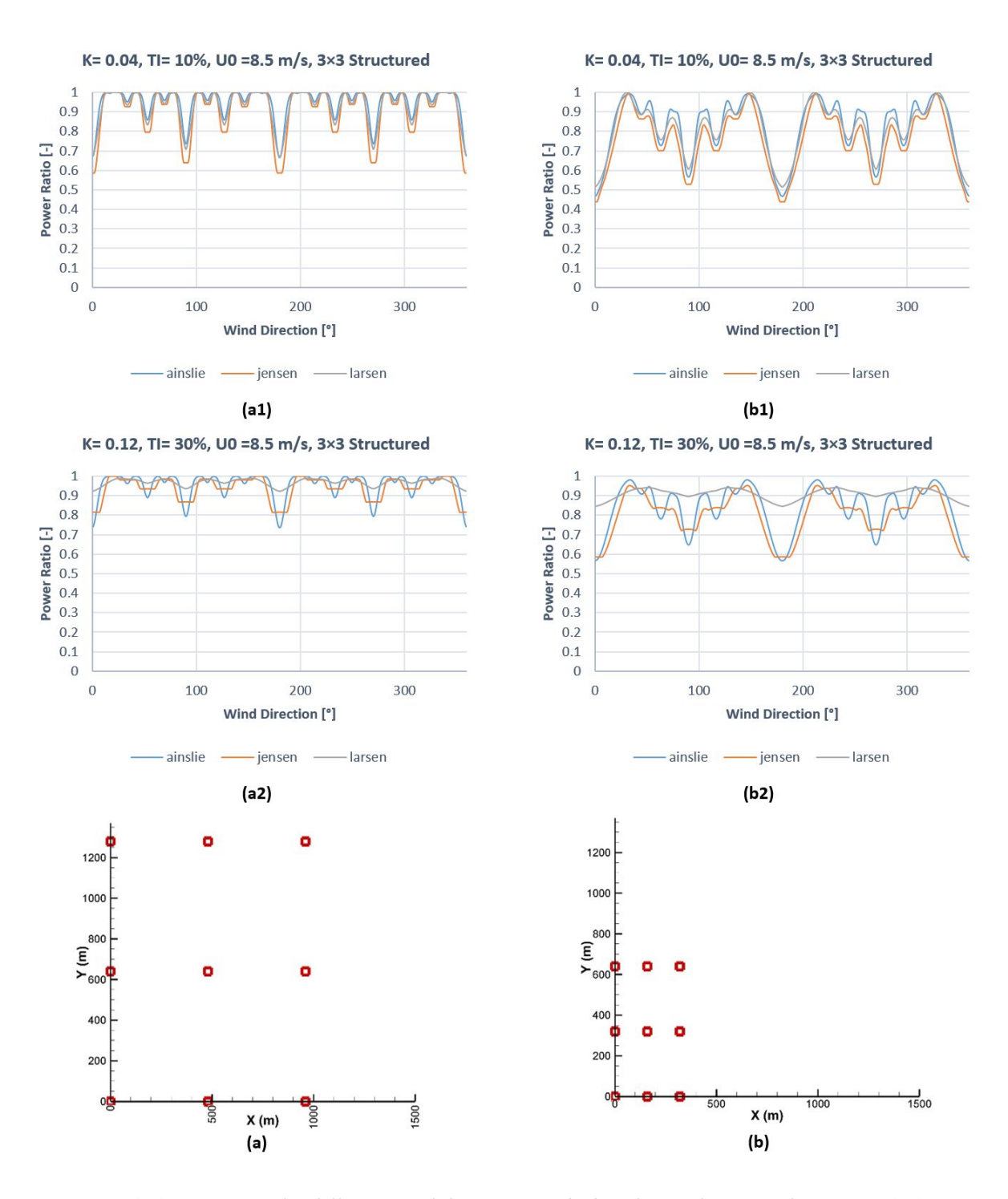


Figure 3.7: (a1) Power ratio for different wind directions in the low density layout and TI = 0.1 - (a2) Power ratio for different wind directions in the low density layout and TI = 0.3 - (a) Low density layout - (b1) Power ratio for different wind directions in the high density layout and TI = 0.1 - (b2) Power ratio for different wind directions in the high density layout and TI = 0.3 - (b) High density layout

The main points that are good to mention here are that:

- Generally, the difference between the models is higher when the distances are lower (denser wind farm). This result is in line with previously seen results in 3.2 bullet 3 and 3.3 bullet 4.
- In low TI, the models are more consistent.
- In low TI and for some directions that more turbines are aligned (for example, 180 degree), Ainslie has a higher power ratio than Larsen in the low density wind farm. However, this is completely opposite for the high density wind farm which means that Larsen has a higher power ratio in these directions. This is in complete agreement with figure 3.3 bullet 3 which shows that Ainslie has a higher center-line velocity than Larsen after 6D when TI = 0.1.
- For the lower TI ,the Jensen has the most conservative results. However, while using TI = 0.3, Ainslie shows the lowest power ratio for some directions where more turbines are aligned (for instance, 180 degree). This could be concluded from the previous finding in figure 3.3 bullet 3 that for TI = 0.3, Jensen has a higher wake center-line velocity than Ainslie.
- Ainslie with high TI still has a higher power ratio than Jensen in some directions where the
  number of aligned turbines is low. This is because, in this case, wake mean velocity becomes
  more important than wake center-line velocity. Therefore, Ainslie that has a higher wake
  mean velocity than Jensen for the high TI (see figure 3.2), shows a higher power ratio value
  in these directions.
- There are some sharp points for the Jensen results. This is related to the fact that the Jensen model has a discontinuity in modeling the wake speed. Therefore, the discontinuity causes turbines to suddenly get in or out of the wake.
- By increasing TI, Larsen shows a really different behavior from the other two models by showing a smooth power ratio curve. Also, it has a higher average power ratio compared to the others. This difference is even more recognizable in high density wind farms (shorter distances). The large increase in wake radius, wake mean velocity, and wake center-line velocity with increasing TI make this behavior of the Larsen model fully predictable (see figures 3.1, 3.2, and 3.3).
- Ainslie is the least sensitive model to variation in TI. Its power ratio curve for the high and the low TI has the least changes relative to other models.

From the results in section 3.3 it several fact could be concluded regarding to the layout optimization. First, for the higher number of turbines, an optimizer (with just considering the AEP) tends to have larger spacing compare to a wind farm with less turbine. But, it might not be true due to the extra costs of larger spacing. Second, a place with higher wind speed average is

better for constructing a wind farm; not only due to the higher energy available in the area, but also due to the less wake losses that accrues in the farm. Moreover, the farm turbines' spacing would be smaller for the higher average wind situation. Third, Larsen may lead to smaller spacing due to its lower power ratio drop for decreasing spacing around 3D region (more visible in high turbulence intensities). Also, for the high TI, Jensen shows higher power ratio decrease than Ainslie by decreasing the spacing (around 3D region) which is opposite to the situation for the lower TI (but not in directions with less aligned turbines).

## 3.4 Wind farm annual energy yield

The following setup has been used in order to study the effect of turbine positioning in a wind farm. For this purpose, an extra turbine is moved along the sinusoidal curves shown in figure 3.8 a and 3.9 a. These results could shed light on the behavior of optimizers as well (see section 2.5.1). Figures 3.8 and 3.9 are illustrating the annual energy yield of the wind farms as function of the added turbine position.

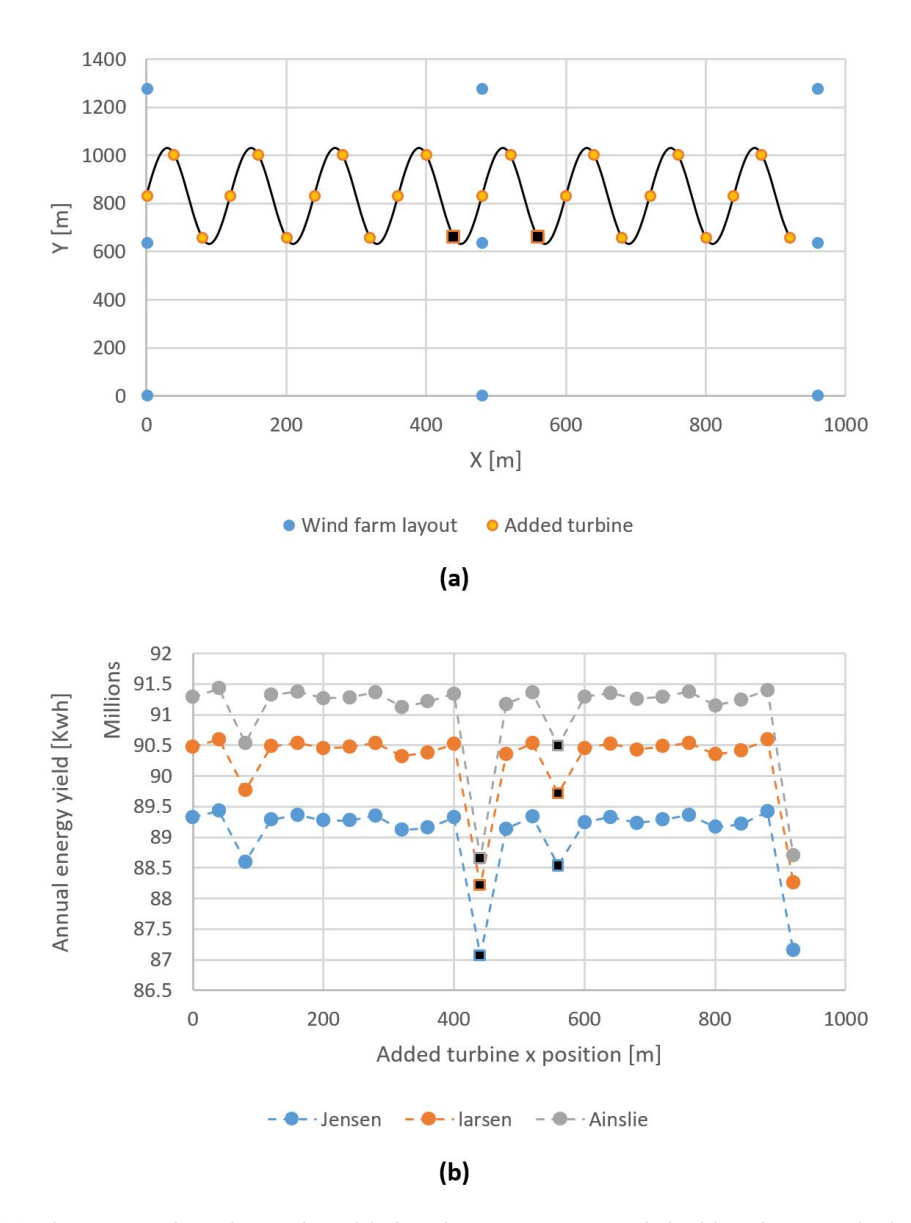


Figure 3.8: (a) The orange dots shows the added turbine positions, and the blue dots are the base wind farm layout - (b) Wind farm AEP as a function of the added turbine (x) positions in the  $3 \times 3$  layout

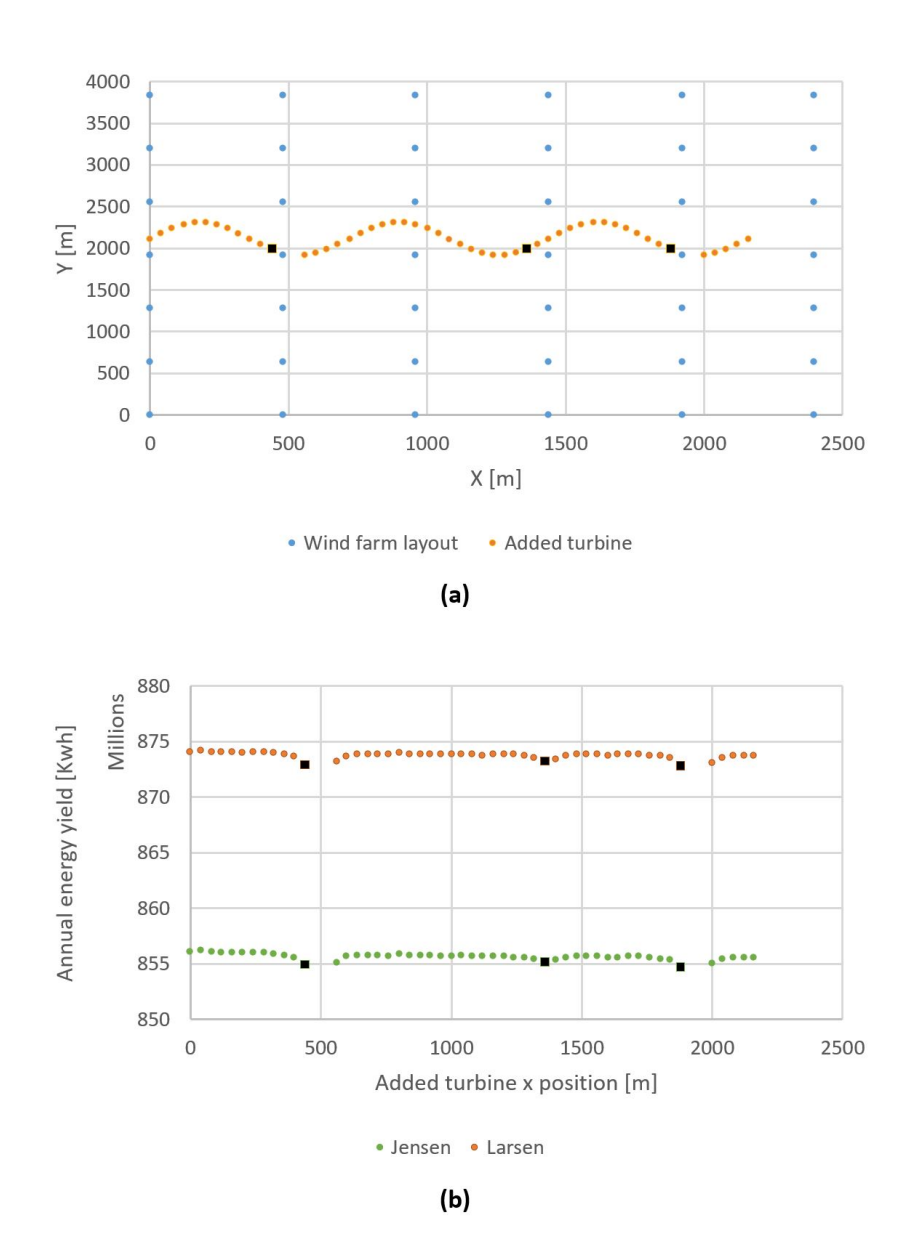


Figure 3.9: (a) The orange dots shows the added turbine positions, and the blue dots are the base wind farm layout (for the better visualization not the whole farm is shown here) - (b) Wind farm AEP as a function of the added turbine (x) positions in the  $10\times10$ 

The interesting point in figures 3.8 and 3.9 is that:

• all the models are showing a similar trend for AEP. For instance, the black dots in these graphs show some local minimum AEP points at the same added turbine positions for all the models.

Annual energy yield of 8 different random layouts is shown in figure 3.10 (check appendix C for the layouts).

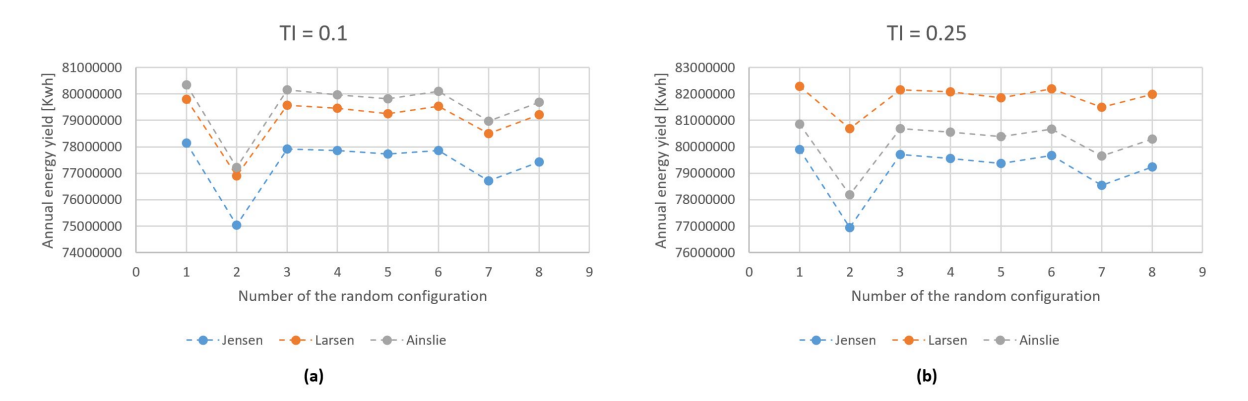


Figure 3.10: Annual energy yield for 8 different random layout with 9 turbines when (a) TI = 0.1, (b) TI = 0.25

This setup again proves that:

 All the models have the same behavior regarding the ranking of layouts based on their AEP.

In table 3.1 annual energy yield of the low density  $3\times 3$  wind farm is shown. These numbers are the most accurate results (AEP for 1 degree direction step, 1m/s speed step, and 0 degree starting point of direction sampling) that have been calculated in the setup shown in tables 3.2 ,3.3, and 3.4. For the ease of comparison, the numbers are divided by the annual energy yield calculated by the Jensen model with TI = 0.1 that has the lowest energy yield (81130853.67 kWh).

 Jensen
 Larsen
 Ainslie

 TI = 0.1
 1
 1.011519476
 1.020149232

1.014997282

Table 3.1: Annual energy yield for the low density  $3\times 3$  wind farm

#### From table 3.1 is observed that:

TI = 0.25

• The Jensen model has the most conservative result compare to other models for both high and low turbulence intensities.

1.026910017

1.022308287

- By increasing the TI from 0.1 to 0.25, Jensen increased by 1.49%, Ainslie increased by 0.2%, and Larsen increased by 1.52%.
- The Ainslie model has the lowest AEP increase by TI (see figure 3.7 last bullet). This causes Larsen to give a higher AEP than Ainslie for the high TI.

- Jensen has a higher growth by TI, but still Ainslie has a larger value when TI = 0.25. This could be explained by the result seen in 3.7 bullet 5 that Ainslie has a higher power ratio than Jensen in directions with lower number of turbines aligned.
- The ranking of the models' AEP were similar to the other setups like those shown in figures 3.8, 3.9, and 3.10.

By looking at figures 3.8, 3.9, and 3.10 and their wind farm layouts when these setups have the lowest AEPs, it could be concluded that:

Although the wind farms have a same total density (within each setup), their annual energy
yield are really sensitive to smallest distance between the turbines. In all of them, the
AEP is the lowest when two ore more turbines are closest to each other compare to other
layouts. So, uniformly spreading turbines in a wind farm is an important factor for turbine
positioning in a wind farm.

Tables 3.2 ,3.3, and 3.4 are showing the annual energy yield for different direction sampling steps, speed sampling steps, and turbulence intensities. Moreover, the starting point of wind direction sampling is varied in these tables to show the accuracy level and sensitivity of AEP calculation with respect to wind direction steps. In order to be able to easily compare these parameters' effects, all numbers in each matrix are divided by the most accurate data for that specific situation in each matrix (AEP for 1 degree direction step, 1 m/s speed step, and 0 degree starting point of direction sampling). For instance, all the numbers for the Jensen AEP matrices with TI = 0.25 are divided by the  $1.014997282 \times 81130853.67kWh$  (see table 3.1).

Table 3.2: Annual energy production matrix using the Jensen model in the  $3\times3$  layout. AEPs have been normalized by the computationally most accurate result which is 1 degree direction sampling step and 1m/s speed step

Jensen	3*3, TI = $0.1$				
	0	0	0	0	Starting point (°)
	30	10	5	1	Direction step (°)
1	0.969207256	1.002571875	1.001223595	1	
3	0.972842332	1.00698072	1.005780112	1.004574091	
7	0.943667284	0.964092466	0.962815039	0.962032373	
21	1.797967495	1.802460685	1.802761902	1.802567323	
Speed step (m/s)					
Jensen	3*3, TI = 0.1				
	15	5	2.5	0.5	Starting point (°)
	30	10	5	1	Direction step (°)
1	1.041537328	0.999875316	0.9986991	0.999939436	
3	1.04592739	1.004579504	1.003263977	1.004513273	
7	0.990774589	0.961537612	0.961242129	0.961991768	
21	1.805808835	1.803063119	1.802298768	1.802549851	
Speed step (m/s)					
Jensen	3*3, TI = 0.25				
	0	0	0	0	Starting point (°)
	30	10	5	1	Direction step (°)
1	0.987675621	1.000261183	0.999935191	1	
3	0.992948032	1.005262887	1.004921845	1.005002204	
7	0.94590069	0.955281775	0.95530475	0.955397586	
21	1.777863236	1.778449249	1.778349707	1.778346187	
Speed step (m/s)					
Jensen	3*3, TI = $0.25$				
	15	5	2.5	0.5	Starting point (°)
	30	10	5	1	Direction step (°)
1	1.017013023	0.999609199	1.000252755	0.999990247	
3	1.021580293	1.004580803	1.005263421	1.004996841	
7	0.968388989	0.955327725	0.955628926	0.95539348	
21	1.779003022	1.778250164	1.778352647	1.778345455	
Speed step (m/s)					

Table 3.3: Annual energy production matrix using the Larsen model in the  $3 \times 3$  layout. AEPs have been normalized by the computationally most accurate result which is 1 degree direction sampling step and 1m/s speed step

Larsen	3*3, TI = 0.1				
	15	5	2.5	0.5	Starting point (°)
	30	10	5	1	Direction step (°)
1	1.027453734	1.000569079	1.000005632	0.999976765	
3	1.031853742	1.005757008	1.004913582	1.004922755	
7	0.977652174	0.958418582	0.958062274	0.958107539	
21	1.785227698	1.783525506	1.783182448	1.783141523	
Speed step (m/s)					
Larsen	3*3, TI = 0.25				
	15	5	2.5	0.5	Starting point (°)
	30	10	5	1	Direction step (°)
1	1.003629833	1.000077332	1.000004039	0.99999757	
3	1.008194925	1.004743683	1.004672771	1.004666565	
7	0.956028907	0.953295165	0.953237072	0.953231596	
21	1.75836564	1.758227077	1.758223106	1.758222569	
Speed step (m/s)					

Table 3.4: Annual energy production matrix using the Ainslie model in the  $3 \times 3$  layout. AEPs have been normalized by the computationally most accurate result which is 1 degree direction sampling step and 1m/s speed step

Ainslie	3*3, TI = $0.1$				
	15	5	2.5	0.5	Starting point (°)
	30	10	5	1	Direction step (°)
1	1.020650136	1.001881934	1.000075416	0.999987891	
3	1.024965037	1.006696423	1.004790822	1.004683405	
7	0.970845022	0.95690339	0.956207109	0.956118922	
21	1.770141833	1.769282759	1.768301268	1.768155793	
Speed step (m/s)					
Ainslie	3*3, TI = 0.25				
	15	5	2.5	0.5	Starting point (°)
	30	10	5	1	Direction step (°)
1	1.018107004	1.00102193	1.000045693	0.999982237	
3	1.022428991	1.005780286	1.004751298	1.00470333	
7	0.968416667	0.955723579	0.955370413	0.955340594	
21	1.766402584	1.765679175	1.765215659	1.765176659	
Speed step (m/s)					

The general points that could be concluded from tables 3.2,3.3, and 3.4 are:

• For all the models, the AEP is more sensitive to the speed step than the direction step. This is due to the fact that the power production is proportional to the cube of wind speed, but the power production is less sensitive to wind direction. For instance, in figure 3.5 the difference in power production of different directions is maximum 40 %.

- By increasing the speed step, all the models show the same level of divergence up to 10 degree direction bins. For instance, all the models show 0.001 order of magnitude deviation when the speed step is increased from 1 m/s to 3 m/s. This is due to the fact that power curve averaging error in these cases is much larger than the direction error; therefore, the speed step is a determining factor for the divergence order of magnitude.
- The direction error for the 30 degree direction step which has 0.01 order of magnitude is large enough to have a determining role in divergence also for the higher than 1m/s speed steps. This is not true for Larsen with TI = 0.25 and 3 m/s speed bins. For this case, Larsen has an order of magnitude lower divergence compared to all different cases with 3 m/s speed step and 30 degree direction step. This has happened due to the fact that Larsen has a small sensitivity to the direction in higher TI. Therefore, the speed step error is still dominating in this case which has 0.001 order of magnitude divergence for the 3 m/s speed step.
- In all the models except Ainslie, for the higher TI, the AEP is relatively less sensitive to the direction sampling step and sampling starting point.
- In general, Larsen has the lowest sensitivity to the wind direction sampling step and starting point, and Jensen has the highest sensitivity, except for the high TI for which Ainslie has the highest sensitivity.

In order to find the number of turbines' effect, the same setup is used but this time for the  $10 \times 10$  layout. The results for TI = 0.1 are shown in table 3.5 and the full table with other turbulence intensity and (direction) starting point is shown in table D.3.

Table 3.5: Annual energy production matrix using the Jensen model in the  $10 \times 10$  layout. AEPs have been normalized by the computationally most accurate result which is 1 degree direction sampling step and 1m/s speed step

Jensen	10*10, TI = $0.1$				
	15	5	2.5	0.5	Starting point (°)
	30	10	5	1	Direction step (°)
1	1.066025271	1.000388604	0.997414083	0.999802539	
3	1.071952747	1.006182356	1.003420365	1.005716728	
7	1.02000005	0.980909078	0.979624611	0.98109992	
21	1.923699726	1.916912234	1.911570229	1.913211427	
Speed step (m/s)					

Comparing table 3.2 and 3.5 shows that:

• The wind direction step and starting point have more influence in the wind farm with higher number of turbines than the smaller farm. This is because the power ratio curve for larger wind farms has more ups and downs which makes it more sensitive to the wind direction (see figure 3.4).

Figure 3.11 shows the ratio and difference of AEPs calculated by the models with each other. This compare is done for figures 3.8 and 3.10 in which the different models have similar trends and it is interesting to investigate whether they have constant difference or differ by a constant factor.

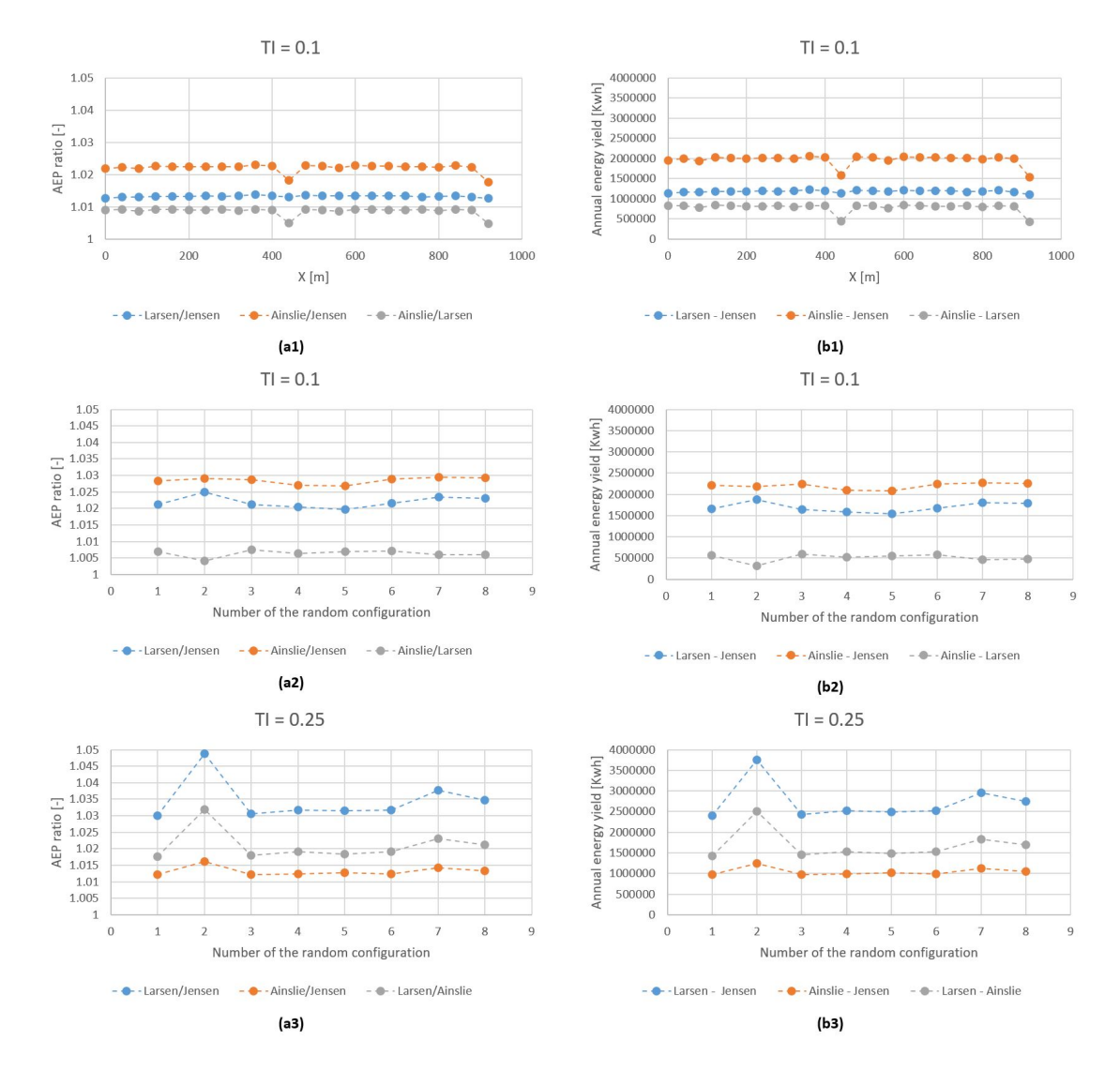


Figure 3.11: (a1) Ratio of AEPs in figure 3.8 - (b1) Difference of AEPs in figure 3.8 - (a2) Ratio of AEPs in figure 3.10 with TI = 0.1 - (b2) Difference of AEPs in figure 3.10 with TI = 0.3 - (a3) Ratio of AEPs in figure 3.10 with TI = 0.1 - (b3) Difference of AEPs in figure 3.10 with TI = 0.3

#### Figure 3.11 shows that:

- Behaviour of the models for the lower TI are more consistent with each other than the higher TI in terms of difference and factor ratio.
- It seems that ratio of AEPs and differences have a relatively constant value which is a function of TI and averaged wind farm density. But, this relatively constant value is really

sensitive to the minimum distance between turbines in the specific setup. For instance, the local minima and maxima in figure 3.11 are happened when some turbines get relatively close to each other (although the wind farm density is constant).

- Figure 3.11 (a2) show (a3) show the decrease in Jensen's AEP by decreasing turbines spacing is larger than Ainslie and Larsen. It should be mentioned that sensitivity of the Jensen model to decreasing turbines distance (less than 3D) is more noticeable for higher TI. Moreover, Ainslie shows more decrease than Larsen. Also, for both high and low TI, Ainslie and Jensen shows more similar behavior in decreasing the AEP (the ratio or difference is more close to a straight line).
- Figure 3.11 (a1) and (b1) illustrate that the Larsen model has the highest decrease in AEP in the local minimum (that happens when the added turbine and the wind farm turbines has the closest position). This behavior is different from previously seen result in which Larsen has the lowest increase. This has happened due to the fact that in this case the distance between the added turbine and the other turbine become closer than 1D, and using far-wake models are not valid. So, the results is not necessarily reliable.

This section is in line with the previously seen results in sections 3.2 and 3.3 that when the Larsen model is used, the optimized layout depend more on TI. Also, using Jensen's model, may lead to larger spacing because it has higher sensitivity to the turbines' distances (mainly for 3D region).

## 4

## CONCLUSION & FUTURE RESEARCH

#### 4.1 Conclusion

The evidence from this study points towards the interesting idea that the WFLO result, would be similar for different wake models when the geometry is defined and there is no cost calculation (the only objective function is annual energy yield). This has been seen in the setups with a random layout wind farm and the randomly added turbine in the farm. In these setups all the models have the same ranking for the farms annual energy yield. Although the models are not showing the same value for the annual energy yield, the general trends of the result and the ranking of the annual energy production for different layouts are identical. Therefore, the output of optimization would be the same for the fastest model (Jensen) and the most time consuming model (Ainslie). This observation is related to two reasons. First, the power ratio curve has shown similar trends for all the wake models in almost all the different cases. Generally, all the models have shown the same ascending or descending pattern with respect to the wind direction almost for the whole 360 degree. Therefore, it could be concluded that all the models are same in pattern but different in numbers or slops (= power ratio to wind direction). So, after the integration for the AEP, all of them show the same pattern but different numbers. Second, The essence of a realistic wind rose would act like a great damper, and averages out some differences in patterns. For instance, for the higher density, Larsen does not follow the large variation in farm power for different wind directions in Jensen and Ainslie. But, if a trend-line fits to the Jensen or Ainslie, it will show a same ascending or descending pattern as Larsen. So, a realistic wind rose has a sort of the same function. It highlights the general behavior of the power ratio curve rather than magnifying the different ups and down for some specific parts. But, this conclusion that WFLO result will be the same for all the models might not be true anymore when a clean narrow predominant wind direction is used (instead of a realistic wind rose). It is also good to mention that it seems that ratio (and differences) of AEPs between the models, have a relatively constant value which is a function of TI and wind farm density. But, this relatively constant value is really sensitive to the minimum distance between turbines in the specific setup. For instance, the AEP reaches the lowest value (for all the models) when the minimum distance between turbines in

a farm (same number of turbines with the same total density but a random configuration) is the lowest compare to other layouts. This is because all the models have a similar pattern in increasing the wake losses closer to a wind turbine (which is more steep closer to the turbine, so the wake losses when getting closer to a nearest turbine are higher than the benefits of getting far from the others). Therefore, all the models represent the mentioned layout as the lowest annual energy yield production. Although all the models agree on the ranking of the AEP for different layouts, the Jensen has the largest decrease in AEP by decreasing the minimum distance between turbines in the farm. This fact would lead optimization process to end up with a larger spacing while using the Jensen model than the other models.

The results have shown that behavior of the wake models are more consistent for lower turbulence intensities and lower wind farm density. Ainslie is the least sensitive model to the turbulence intensity and Larsen is the most sensitive model to it. Models inconsistency increases by increasing the number of turbines, and also make the calculation more sensitive to the wind direction step size. Larsen is the least sensitive model to the wind direction step size and Jensen is the most sensitive model. Also, it has been figured out that the effect of wind speed step size is more dominant than wind direction step size. Therefore, it is important to consider logical steps size for both parameters in order to avoid high calculation times and not getting accurate enough results.

## 4.2 Future Research

For the future research it is good to investigate effects of atmospheric stability and increased turbulence intensity due to wakes in annual energy production and optimization process. Moreover, wind-rose has shown a great averaging effect during the annual energy yield calculation, but its effects has not been studied in detail during this project. Therefore, focusing more on wind-rose accuracy (compare to real situation), wind-rose bin size, wind-rose shape (e.g. be more uniform in all directions or has a a clean narrow predominant wind direction), etc. would be useful to better understand the other parameters level of influence on annual energy yield calculation after integrating the power outputs for different wind directions.

Also, this study could be the basis of future research in order to provide a guideline for WFLO. This guideline should be consist of all the modeling parameters relative inaccuracy size and suggests a rational combination of the parameters in order to avoid killing time on pre-known inaccurate result. These parameters could be wind direction step size accuracy, wind speed step size accuracy, wake model accuracy regarding to the turbulence intensity, wind-rose bin size accuracy, etc.

In the end, following these investigated setups with optimization process would be necessary to confirm the findings in this project.

## **BIBLIOGRAPHY**

- [1] K. Dykes, R. Meadows, F. Felker, P. Graf, M. Hand, M. Lunacek, J. Michalakes, P. Moriarty, W. Musial, and P. Veers, *Applications of systems engineering to the research, design, and development of wind energy systems*. National Renewable Energy Laboratory, 2011.
- [2] J. S. González, M. B. Payán, J. M. R. Santos, and F. González-Longatt, "A review and recent developments in the optimal wind-turbine micro-siting problem," *Renewable and Sustainable Energy Reviews*, vol. 30, pp. 133–144, 2014.
- [3] M. Ali, J. Matevosyan, and J. Milanović, "Probabilistic assessment of wind farm annual energy production," *Electric Power Systems Research*, vol. 89, pp. 70–79, 2012.
- [4] M. Stevens and P. Smulders, "The estimation of the parameters of the weibull wind speed distribution for wind energy utilization purposes," *Wind engineering*, pp. 132–145, 1979.
- [5] N. Eskin, H. Artar, and S. Tolun, "Wind energy potential of gökçeada island in turkey," Renewable and Sustainable Energy Reviews, vol. 12, no. 3, pp. 839–851, 2008.
- [6] C. Justus, W. Hargraves, A. Mikhail, and D. Graber, "Methods for estimating wind speed frequency distributions," *Journal of applied meteorology*, vol. 17, no. 3, pp. 350–353, 1978.
- [7] J. A. Carta, P. Ramirez, and S. Velazquez, "A review of wind speed probability distributions used in wind energy analysis: Case studies in the canary islands," *Renewable and Sustainable Energy Reviews*, vol. 13, no. 5, pp. 933–955, 2009.
- [8] F. M. Gonzalez-Longatt, P. Wall, P. Regulski, and V. Terzija, "Optimal electric network design for a large offshore wind farm based on a modified genetic algorithm approach," *IEEE Systems Journal*, vol. 6, no. 1, pp. 164–172, 2012.
- [9] S. Lumbreras and A. Ramos, "Offshore wind farm electrical design: a review," *Wind Energy*, vol. 16, no. 3, pp. 459–473, 2013.
- [10] G. Quinonez-Varela, G. Ault, O. Anaya-Lara, and J. McDonald, "Electrical collector system options for large offshore wind farms," *IET Renewable Power Generation*, vol. 1, no. 2, pp. 107–114, 2007.
- [11] K. Nassar, M. El Masry, and H. Osman, "Simulating the effect of access road route slection on wind farm construction," in *Simulation Conference (WSC)*, Proceedings of the 2010 Winter. IEEE, 2010, pp. 3272–3282.
- [12] J. D. Sørensen, "Optimal, reliability-based turbine placement in offshore wind turbine parks," Civil Engineering and Environmental Systems, vol. 24, no. 2, pp. 99–109, 2007.

- [13] P. Tavner, C. Edwards, A. Brinkman, and F. Spinato, "Influence of wind speed on wind turbine reliability," *Wind Engineering*, vol. 30, no. 1, pp. 55–72, 2006.
- [14] O. Ozgener and L. Ozgener, "Exergy and reliability analysis of wind turbine systems: a case study," *Renewable and Sustainable Energy Reviews*, vol. 11, no. 8, pp. 1811–1826, 2007.
- [15] I. D. Bishop and D. R. Miller, "Visual assessment of off-shore wind turbines: The influence of distance, contrast, movement and social variables," *Renewable Energy*, vol. 32, no. 5, pp. 814–831, 2007.
- [16] J. P. Hurtado, J. Fernández, J. L. Parrondo, and E. Blanco, "Spanish method of visual impact evaluation in wind farms," *Renewable and Sustainable Energy Reviews*, vol. 8, no. 5, pp. 483–491, 2004.
- [17] J. Ladenburg, "Visual impact assessment of offshore wind farms and prior experience," *Applied Energy*, vol. 86, no. 3, pp. 380–387, 2009.
- [18] A. Crespo, J. Hernandez, and S. Frandsen, "Survey of modelling methods for wind turbine wakes and wind farms," *Wind energy*, vol. 2, no. 1, pp. 1–24, 1999.
- [19] E. Bossanyi, G. Whittle, P. Dunn, N. Lipman, P. Musgrove, and C. Maclean, "The efficiency of wind turbine clusters," in 3rd International symposium on wind energy systems, 1980, pp. 401–416.
- [20] R. J. Templin, "An estimation of the interaction of windmills in widespread arrays," National Aeronautical Establishment, Ottawa, Tech. Rep. Laboratory Report LTR-LA-171, 1974.
- [21] B. Newman, "The spacing of wind turbines in large arrays," *Energy conversion*, vol. 16, no. 4, pp. 169–171, 1977.
- [22] C. Crafoord, "Interaction in limited arrays of windmills," NASA STI/Recon Technical Report N, vol. 83, 1979.
- [23] D. Moore, "Depletion of available wind power by a large network of wind generators," in *International Conference on Future Energy Concepts*, 1979, pp. 302–305.
- [24] S. Emeis and S. Frandsen, "Reduction of horizontal wind speed in a boundary layer with obstacles," *Boundary-Layer Meteorology*, vol. 64, no. 3, pp. 297–305, 1993.
- [25] L. Vermeer, J. N. Sørensen, and A. Crespo, "Wind turbine wake aerodynamics," *Progress in aerospace sciences*, vol. 39, no. 6, pp. 467–510, 2003.
- [26] B. Sanderse, "Aerodynamics of wind turbine wakes," *Energy Research Center of the Netherlands (ECN), ECN-E-09-016, Petten, The Netherlands, Tech. Rep*, vol. 5, no. 15, p. 153, 2009.

- [27] H. Snel, "Review of the present status of rotor aerodynamics," *Wind Energy*, vol. 1, no. s 1, pp. 46–69, 1998.
- [28] M. O. L. Hansen, J. N. Sørensen, S. Voutsinas, N. Sørensen, and H. A. Madsen, "State of the art in wind turbine aerodynamics and aeroelasticity," *Progress in aerospace sciences*, vol. 42, no. 4, pp. 285–330, 2006.
- [29] B. Sanderse, S. Pijl, and B. Koren, "Review of computational fluid dynamics for wind turbine wake aerodynamics," *Wind energy*, vol. 14, no. 7, pp. 799–819, 2011.
- [30] H. Snel, "Review of aerodynamics for wind turbines," *Wind energy*, vol. 6, no. 3, pp. 203–211, 2003.
- [31] R. Shakoor, M. Y. Hassan, A. Raheem, and Y.-K. Wu, "Wake effect modeling: A review of wind farm layout optimization using jensen s model," *Renewable and Sustainable Energy Reviews*, vol. 58, pp. 1048–1059, 2016.
- [32] T. Göçmen, P. Van der Laan, P.-E. Réthoré, A. P. Diaz, G. C. Larsen, and S. Ott, "Wind turbine wake models developed at the technical university of denmark: A review," *Renewable and Sustainable Energy Reviews*, vol. 60, pp. 752–769, 2016.
- [33] D. J. Renkema, "Validation of wind turbine wake models," *Master of Science Thesis, Delft University of Technology*, vol. 19, 2007.
- [34] D. R. VanLuvanee, "Investigation of observed and modeled wake effects at horns rev using windpro," *Technical University of Denmark Department of Mechanical Engineering*, 2006.
- [35] F. Seim, "Validating kinematic wake models in complex terrain using cfd," Master's thesis, Norwegian University of Life Sciences, Ås, 2015.
- [36] S. Jeon, B. Kim, and J. Huh, "Comparison and verification of wake models in an onshore wind farm considering single wake condition of the 2 mw wind turbine," *Energy*, vol. 93, pp. 1769–1777, 2015.
- [37] T. Sørensen, M. L. Thøgersen, P. Nielsen, and N. Jernesvej, "Adapting and calibration of existing wake models to meet the conditions inside offshore wind farms," *EMD International A/S. Aalborg*, 2008.
- [38] P. Lissaman, "Energy effectiveness of arbitrary arrays of wind turbines," *J. Energy*, vol. 3, no. 6, pp. 323–328, 1979.
- [39] I. Katic, J. Højstrup, and N. O. Jensen, "A simple model for cluster efficiency," in *European wind energy association conference and exhibition*, 1986, pp. 407–410.
- [40] "Wind energy industry-standard software wasp." [Online]. Available: http://www.wasp.dk/

- [41] [Online]. Available: https://www.windsim.com/products/windsim-brochures.aspx
- [42] "meteodyn forecast software wind production forecast." [Online]. Available: https://meteodyn.com/en/logiciels/cfd-statistical-wind-power-forcasting-software/#.WeeXN2iCxPY
- [43] A. Kusiak and Z. Song, "Design of wind farm layout for maximum wind energy capture," *Renewable Energy*, vol. 35, no. 3, pp. 685–694, 2010.
- [44] G. Mosetti, C. Poloni, and B. Diviacco, "Optimization of wind turbine positioning in large windfarms by means of a genetic algorithm," *Journal of Wind Engineering and Industrial Aerodynamics*, vol. 51, no. 1, pp. 105–116, 1994.
- [45] C. Kiranoudis, N. Voros, and Z. Maroulis, "Short-cut design of wind farms," *Energy Policy*, vol. 29, no. 7, pp. 567–578, 2001.
- [46] U. A. Ozturk and B. A. Norman, "Heuristic methods for wind energy conversion system positioning," *Electric Power Systems Research*, vol. 70, no. 3, pp. 179–185, 2004.
- [47] S. Grady, M. Hussaini, and M. M. Abdullah, "Placement of wind turbines using genetic algorithms," *Renewable energy*, vol. 30, no. 2, pp. 259–270, 2005.
- [48] G. Marmidis, S. Lazarou, and E. Pyrgioti, "Optimal placement of wind turbines in a wind park using monte carlo simulation," *Renewable energy*, vol. 33, no. 7, pp. 1455–1460, 2008.
- [49] C. N. Elkinton, J. F. Manwell, and J. G. McGowan, "Optimizing the layout of offshore wind energy systems," *Marine Technology Society Journal*, vol. 42, no. 2, pp. 19–27, 2008.
- [50] S. Şişbot, Ö. Turgut, M. Tunç, and Ü. Çamdalı, "Optimal positioning of wind turbines on gökçeada using multi-objective genetic algorithm," *Wind Energy*, vol. 13, no. 4, pp. 297–306, 2010.
- [51] J. S. González, A. G. G. Rodriguez, J. C. Mora, J. R. Santos, and M. B. Payan, "Optimization of wind farm turbines layout using an evolutive algorithm," *Renewable energy*, vol. 35, no. 8, pp. 1671–1681, 2010.
- [52] J. S. González, Á. G. Rodríguez, J. C. Mora, M. B. Payán, and J. R. Santos, "Overall design optimization of wind farms," *Renewable Energy*, vol. 36, no. 7, pp. 1973–1982, 2011.
- [53] B. Saavedra-Moreno, S. Salcedo-Sanz, A. Paniagua-Tineo, L. Prieto, and A. Portilla-Figueras, "Seeding evolutionary algorithms with heuristics for optimal wind turbines positioning in wind farms," *Renewable Energy*, vol. 36, no. 11, pp. 2838–2844, 2011.

- [54] Y. Eroğlu and S. U. Seçkiner, "Design of wind farm layout using ant colony algorithm," *Renewable Energy*, vol. 44, pp. 53–62, 2012.
- [55] C. Wan, J. Wang, G. Yang, H. Gu, and X. Zhang, "Wind farm micro-siting by gaussian particle swarm optimization with local search strategy," *Renewable Energy*, vol. 48, pp. 276–286, 2012.
- [56] W. Y. Kwong, P. Y. Zhang, D. Romero, J. Moran, M. Morgenroth, and C. Amon, "Wind farm layout optimization considering energy generation and noise propagation," in ASME 2012 International Design Engineering Technical Conferences and Computers and Information in Engineering Conference, American Society of Mechanical Engineers, DETC2012-71478, vol. 323332, 2012.
- [57] "Windfarmer." [Online]. Available: https://www.dnvgl.com/services/windfarmer-3766
- [58] "Windpro." [Online]. Available: https://www.emd.dk/WindPRO/
- [59] "Openwind: Wind farm design software aws software." [Online]. Available: http://software.awstruepower.com/openwind/
- [60] S. Sanchez Perez-Moreno, "Model fidelity selection for multi-disciplinary design analysis and optimisation of offshore wind farms," Wind energy department of TU Delft, Tech. Rep., 2016, supervisors: Michiel Zaaijer and Gerard van Bussel.
- [61] J. Choi and M. Shan, "Advancement of jensen (park) wake model," in *Proceedings of the European Wind Energy Conference and Exhibition*, 2013, pp. 1–8.
- [62] T. Gögmen, "Possible power estimation of down-regulated offshore wind power plants," Ph.D. dissertation, Technical University of Denmark, 2016.
- [63] M. P. C. Bontekoning, "Analysis of the reduced wake effect for available wind power calculation during curtailment-including validation experiments," Master's thesis, NTNU, 2017.
- [64] J. F. Ainslie, "Calculating the flowfield in the wake of wind turbines," Journal of Wind Engineering and Industrial Aerodynamics, vol. 27, no. 1-3, pp. 213–224, 1988.
- [65] M. Anderson, "Simplified solution to the eddy-viscosity wake model," *Document prepared by Renewable Energy Systems Ltd ("RES")*, 2009.
- [66] G. C. Larsen, A simple wake calculation procedure, 1988.
- [67] E. Djerf and H. Mattsson, "Evaluation of the software program windfarm and comparisons with measured data from alsvik," *The aeronautical research institute of Sweden*, 2000.



The wind turbine that is used in the modelling is V90-2.0 MW from the Vestas company . The V90 specification, modelling assumptions, thrust coefficient, and power coefficient are shown in table A.1 and figure A.1.

Table A.1: V90-2MW technical specifications

Rated power	2000 kW
Cut-in wind speed	4 m/s
Cut-out wind speed	25 m/s
Rotor radius	40 m
Hub height	100 m

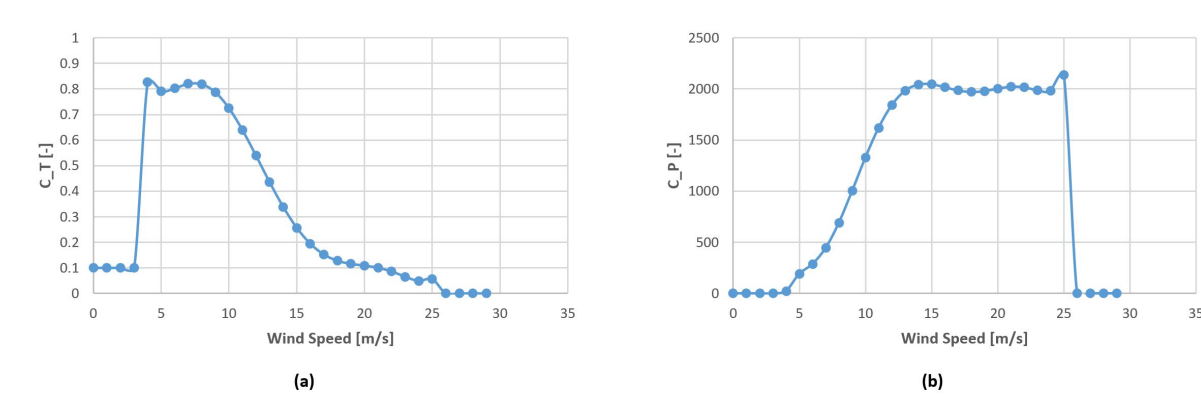
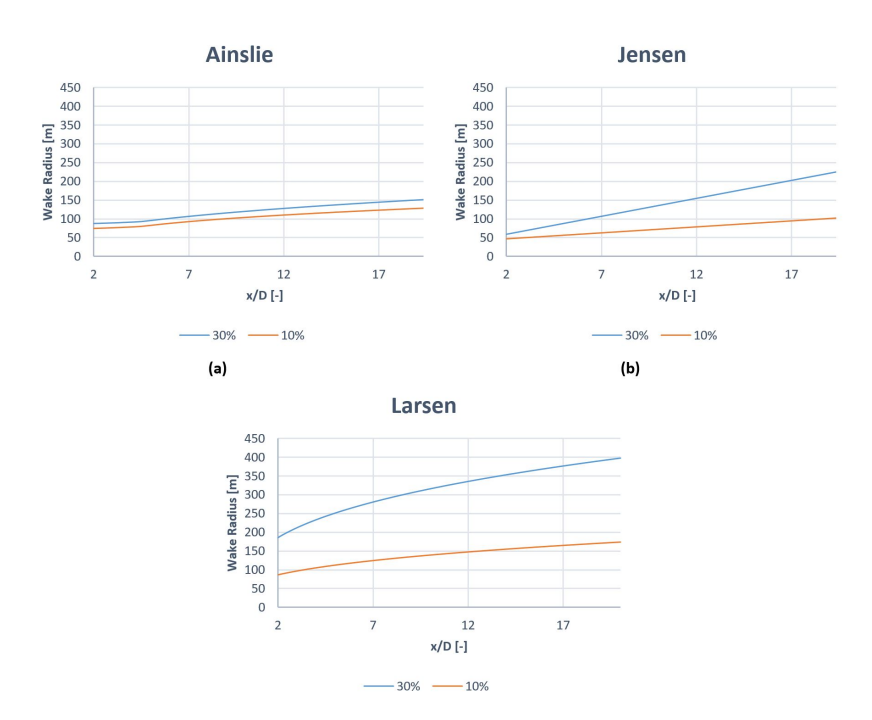


Figure A.1: V90 (a) Thrust coefficient - (b) Power coefficient



Here, figures 3.1, 3.2, and 3.3 are represented in different arrangement in order to make it easier for comparing the behavior of each model with itself while increasing the TI.



Figure~B.1: Downstream~wake~radius~for~TI:~0.1~and~0.3~by~(a)~Ainslie~-~(b)~Jesnen~-~(c)~Larsen~Ainslie~-~(b)~Jesnen~-~(c)~Larsen~-~(

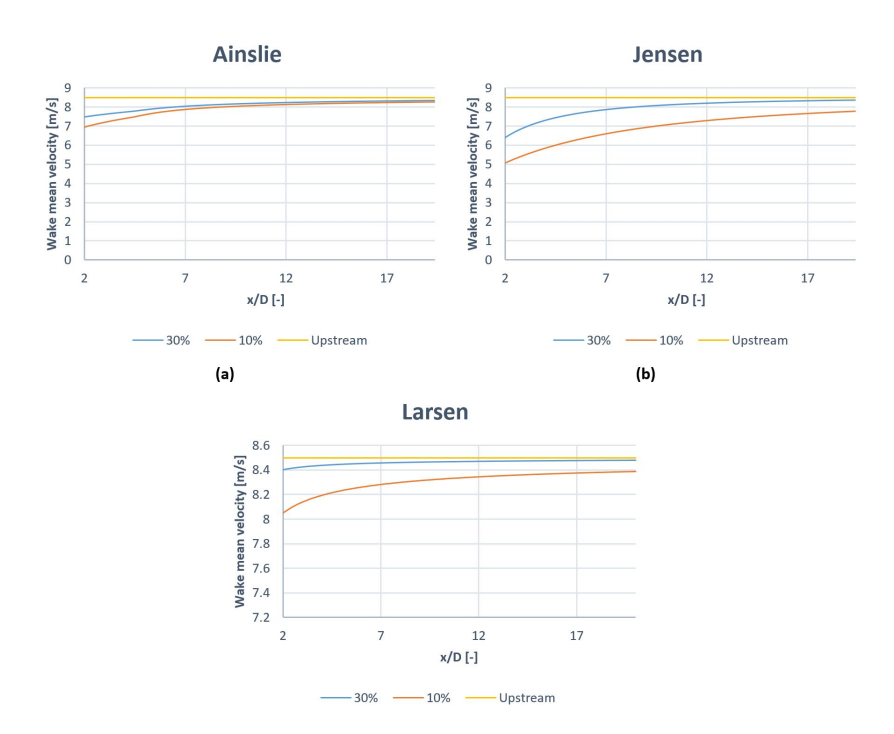
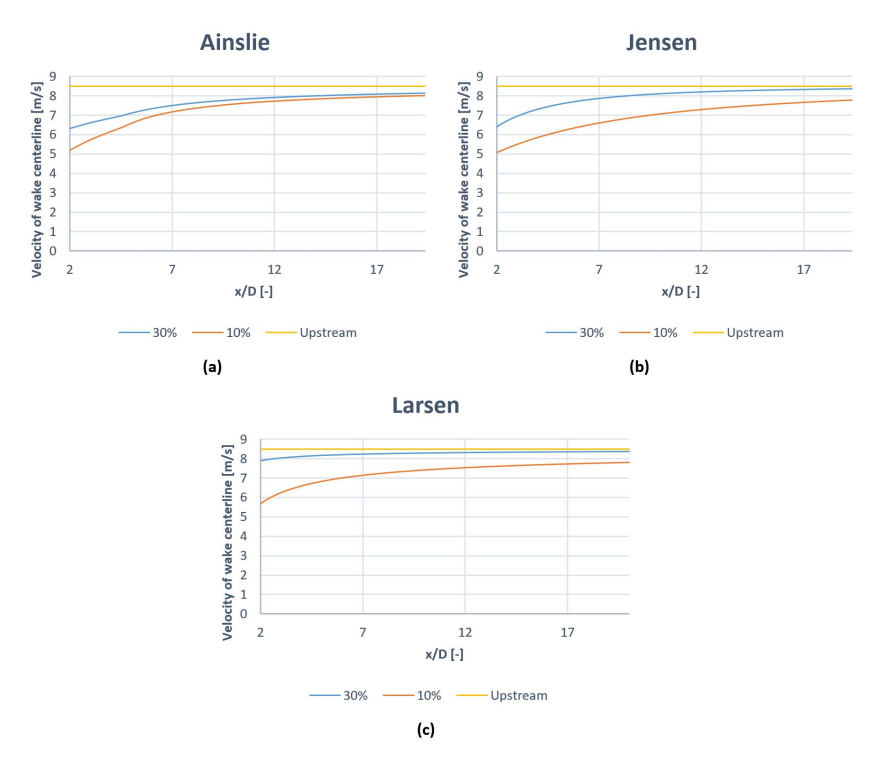


Figure B.2: Downstream wake mean velocity for TI: 0.1 and 0.3 by (a) Ainslie - (b) Jesnen - (c) Larsen



Figure~B.3: Downstream~wake~center-line~velocity~for~TI:~0.1~and~0.3~by~(a)~Ainslie~-~(b)~Jesnen~-~(c)~Larsen~Ainslie~-~(b)~Jesnen~-~(c)~Larsen~-~



## The random layouts using in figure 3.10 are :

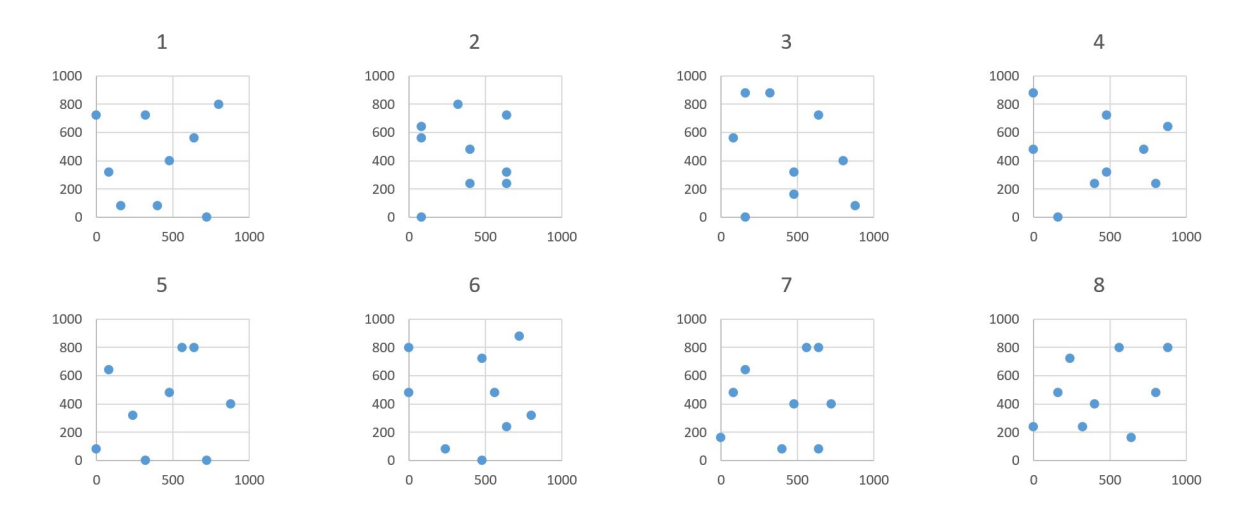


Figure C.1: Downstream wake mean velocity for TI: 0.1 and 0.3 by (a) Ainslie - (b) Jesnen - (c) Larsen

All the numbers are in meter.



Table D.1: Annual energy production ratio matrix using the Larsen model in the  $3\times3$  layout. AEPs have been divided by the computationally most accurate result which is 1 degree direction sampling step and 1m/s speed step

Larsen	3*3, TI = 0.1				
	15	5	2.5	0.5	Starting point (°)
	30	10	5	1	Direction step (°)
1	1.027453734	1.000569079	1.000005632	0.999976765	
3	1.031853742	1.005757008	1.004913582	1.004922755	
7	0.977652174	0.958418582	0.958062274	0.958107539	
21	1.785227698	1.783525506	1.783182448	1.783141523	
Speed step (m/s)	1				
Larsen	3*3, TI = 0.1				
	0	0	0	0	Starting point (°)
	30	10	5	1	Direction step (°)
1	0.97356397	0.999420105	0.999994592	1	
3	0.978383024	1.004238988	1.004997998	1.004942011	
7	0.941336943	0.958003092	0.958210837	0.958122932	
21	1.779045446	1.782693174	1.78310934	1.783145626	
Speed step (m/s)					
Larsen	3*3, TI = 0.25				
	15	5	2.5	0.5	Starting point (°)
	30	10	5	1	Direction step (°)
1	1.003629833	1.000077332	1.000004039	0.99999757	
3	1.008194925	1.004743683	1.004672771	1.004666565	
7	0.956028907	0.953295165	0.953237072	0.953231596	
21	1.75836564	1.758227077	1.758223106	1.758222569	
Speed step (m/s)					
Larsen	3*3, TI = $0.25$				
	0	0	0	0	Starting point (°)
	30	10	5	1	Direction step (°)
1	0.996121408	0.999926827	1.00000208	1	
3	1.00090329	1.004598185	1.004670934	1.0046689	
7	0.950240208	0.953180784	0.953237974	0.953234195	
21	1.758067863	1.758218975	1.758223026	1.758222798	
Speed step (m/s)					

Table D.2: Annual energy production ratio matrix using the Ainslie model in the  $3\times3$  layout. AEPs have been divided by the computationally most accurate result which is 1 degree direction sampling step and 1m/s speed step

Ainslie	3*3, TI = $0.1$				
	15	5	2.5	0.5	Starting point (°)
	30	10	5	1	Direction step (°)
1	1.020650136	1.001881934	1.000075416	0.999987891	
3	1.024965037	1.006696423	1.004790822	1.004683405	
7	0.970845022	0.95690339	0.956207109	0.956118922	
21	1.770141833	1.769282759	1.768301268	1.768155793	
Speed step (m/s)					
Ainslie	3*3, TI = 0.1				
	0	0	0	0	Starting point (°)
	30	10	5	1	Direction step (°)
1	0.971986801	0.998235749	1.000058841	1	
3	0.976615534	1.002813306	1.004754864	1.004718452	
7	0.938768108	0.955390426	0.956146908	0.956141781	
21	1.760995509	1.766846852	1.768064805	1.768167257	
Speed step (m/s)					
Ainslie	3*3, TI = 0.25				
	15	5	2.5	0.5	Starting point (°)
	30	10	5	1	Direction step (°)
1	1.018107004	1.00102193	1.000045693	0.999982237	
3	1.022428991	1.005780286	1.004751298	1.00470333	
7	0.968416667	0.955723579	0.955370413	0.955340594	
21	1.766402584	1.765679175	1.765215659	1.765176659	
Speed step (m/s)					
Ainslie	3*3, TI = $0.25$				
	0	0	0	0	Starting point (°)
	30	10	5	1	Direction step (°)
1	0.978280976	0.999127189	1.00007456	1	
3	0.983263861	1.003808925	1.004794605	1.004730297	
7	0.941550096	0.955082303	0.955402941	0.955358498	
21	1.761734499	1.764650827	1.765165001	1.765182205	
41					

Table D.3: Annual energy production ratio matrix using the Jensen model in the  $10 \times 10$  layout. AEPs have been divided by the computationally most accurate result which is 1 degree direction sampling step and 1m/s speed step

Jensen	10*10, TI = 0.1				
	15	5	2.5	0.5	Starting point (°)
	30	10	5	1	Direction step (°)
1	1.066025271	1.000388604	0.997414083	0.999802539	
3	1.071952747	1.006182356	1.003420365	1.005716728	
7	1.02000005	0.980909078	0.979624611	0.98109992	
21	1.923699726	1.916912234	1.911570229	1.913211427	
Speed step (m/s)					
Jensen	10*10, TI = 0.1				
	0	0	0	0	Starting point (°)
	30	10	5	1	Direction step (°)
1	0.957846221	1.006118318	1.003253461	1	
3	0.96296567	1.011950223	1.00906629	1.00591571	
7	0.960611394	0.985536347	0.983222712	0.981189323	
21	1.913322579	1.911973596	1.914442915	1.913322579	
Speed step (m/s)					
Jensen	10*10, TI = $0.25$				
	15	5	2.5	0.5	Starting point (°)
	30	10	5	1	Direction step (°)
1	1.024744207	0.999017655	1.000436546	0.999986686	
3	1.029945545	1.004816044	1.00629444	1.005814052	
7	0.977892548	0.960203275	0.960886195	0.960493176	
21	1.824898004	1.823502183	1.823722451	1.823698216	
Speed step (m/s)					
Jensen	10*10, TI = 0.25				
	0	0	0	0	Starting point (°)
	30	10	5	1	Direction step (°)
1	0.981260775	1.000405283	0.999711469	1	
3	0.987517988	1.006247818	1.005531931	1.00582377	
7	0.947132106	0.96022477	0.960214023	0.960498091	
21	1.822778427	1.823888213	1.823695198	1.823699532	
Speed step (m/s)					